TurboID Reveals Nek2A's Semi-Dynamic Cell Cycle Interactions and Nusap1 as a novel partner

by

Enes Çiçek

A Dissertation Submitted to the
Graduate School of Health Sciences
in Partial Fulfillment of the Requirements for
the Degree of

Master of Science

in

Cellular and Molecular Medicine

KOÇ
ÜNİVERSİTESİ

15.09.2023

TurboID Reveals Nek2A's Semi-Dynamic Cell Cycle Interactions and Nusap1 as a novel partner

Koç University

Graduate School of Health Sciences

This is to certify that I have examined this copy of a master's thesis by

Enes Çiçek

and have found that it is complete and satisfactory in all respects,
and that any and all revisions required by the final
examining committee have been made.

Committee Members:

_____

Prof. Ceyda Açılan Ayhan (Advisor)

_____

Prof. Nurhan Özlü

_____

Prof. Jay Gopalakrishnan

Date: _____

For my loved ones

ABSTRACT

TurboID Reveals Nek2A's Semi-Dynamic Cell Cycle Interactions and Nusap1 as a novel partner

Enes Cicek

Master of Science in Cellular and Molecular Medicine

18.09.2023

Nek2A is a cell cycle regulated kinase, which is involved in several cellular processes and overexpressed in numerous cancer types. It has been associated with chromosome instability, increased cell proliferation and drug resistance in cancers.

Our study primarily aims to identify the specific partners that interact with Nek2A during the cell cycle, deepening our understanding of Nek2's role in cancer. To meet this objective, we employed the TurboID proximity labeling technique on synchronized cell groups, exploring the dynamic interactions of Nek2A as the cell cycle advances. We synchronized the cells using a double thymidine block and harvested them at designated release time points, focusing on G1/S, late S, and G2/M cell cycle phases. Through mass spectrometry, we identified biotinylated proteins, which we further analyzed using MaxQuant, Cassiopeia, and Amica tools. Our experiments reliably identified previously recognized Nek2A partners like the Anaphase Promoting Complex (APC) and Kif24. We confirmed proteins closely interacting with Nek2A during the G1/S, late S, and G2/M stages using western blotting. Co-immunoprecipitation unveiled direct interactions of Nek2A with proteins such as Nusap1, Kif2c, Mapre3, and Mpg. We also confirmed the colocalization of these proteins with Nek2A using fluorescence microscopy. We took a special interest in Nusap1 due to its unique role, distinct from other Nek2A partners. Nusap1 acts as a stabilizer for DNA damage proteins, and its depletion can lead to DNA strand breaks, negatively impacting cell survival.

Our analysis highlighted a prevalent occurrence of ubiquitin-driven proteolysis during the cell cycle's progression. We initially studied Nusap1's expression in cells with either diminished or amplified Nek2A activity. Remarkably, there was an increase in Nusap1 levels post-siRNA treatment and in two distinct Nek2 null (KO) cell variants. Conversely, overexpression of Nek2A led to a short-lived reduction in Nusap1 amounts, lasting just 6 hours, before other cell mechanisms presumably balanced it. Using the well-known proteasome inhibitor, MG132, we were able to counteract this reduction. Moreover, we observed a notable reduction in Nusap1 ubiquitination in Nek2A KO cells, pointing to the possible role of proteasomal breakdown processes. A broad protein analysis in Nek2A deficient cells confirmed many proteins, including Nusap1, showed decreased expression.

In essence, our findings indicate Nusap1 as a new Nek2A partner, with Nek2A possibly affecting Nusap1's degradation through ubiquitination. The exact nature of this interaction and the clinical significance require further exploration.

ÖZETÇE

TurboID ile Nek2A'nın Yarı-Dinamik Hücre Döngüsü Etkileşimlerinin bulunması ve Nusap1'in Yeni Bir Partner Olarak İncelenmesi.

Enes Çiçek

Hücresel ve Moleküler Tıp, Yüksek Lisans

18.09.2023

Nek2A, hücre döngüsünde düzenlenen bir kinazdır ve birçok hücresel süreçte yer alırken birçok kanser türünde aşırı üretildiği gözlenmiştir. Nek2'nin kanser üzerindeki rolünü derinlemesine anlamamıza yardımcı olacak olan çalışmamızın başlıca amacı, hücre döngüsü sırasında Nek2A ile etkileşime giren özel partnerleri belirlemektir. Bu amaca ulaşmak için TurboID biyotinleme tekniğini senkronize hücre grupları üzerinde kullanarak, hücre döngüsünün ilerledikçe Nek2A'nın dinamik etkileşimlerini inceledik. Hücrele döngüsünü çift timidin blok yöntemini kullanarak durdurduk ve G1/S, geç S ve G2/M hücre döngüsü evrelerine odaklanarak belirli aralıklarla topladık. Kütle spektrometrisi kullanarak biotinilenmiş proteinleri tanımladık ve bunları MaxQuant, Cassiopeia ve Amica araçlarıyla analiz ettik. Deneylerimiz, daha önce tanınmış Nek2A partnerleri olan Anafazı Teşvik Edici Kompleks (APC) ve Kif24 gibi proteinleri güvenilir bir şekilde tanımladı. Nek2A'nın G1/S, geç S ve G2/M evrelerinde yakından etkileşimde bulunduğu proteinleri western blotlama kullanarak doğruladık. Ko-immünopresipitasyon, Nek2A'nın Nusap1, Kif2c, Mapre3 ve Mpg gibi proteinlerle doğrudan etkileşimlerini ortaya çıkardı. Bu proteinlerin Nek2A ile ko-lokalizasyonunu floresan mikroskopi kullanarak doğruladık. Nek2A partnerlerinden farklı bir rol üstlenen Nusap1'e özel bir ilgi gösterdik. Nusap1, DNA hasarı proteinlerinin stabilizatörü olarak çalışır ve onun azalması DNA iplikçik kırıklarına yol açarak hücrenin hayatta kalmasını olumsuz etkileyebilir.

Analizlerimiz, hücre döngüsünün ilerlemesi sırasında ubikitinleme tarafından yönlendirilen proteolizin yaygın bir şekilde meydana geldiğini gösterdi. İlk olarak, Nek2A aktivitesi azalmış veya artmış hücrelerde Nusap1'in protein miktarını inceledik. İlginç bir şekilde, siRNA tedavisi sonrasında ve iki farklı Nek2 null (KO) hücre varyantında Nusap1 seviyelerinde artış gözledik. Nek2A'nın aşırı ifadesi ise, diğer hücre mekanizmalarının muhtemelen dengelenmesi öncesinde yalnızca 6 saat süren Nusap1 miktarında bir kısa süreli azalmaya neden oldu. Bu azalmayı MG132 adlı iyi bilinen proteazom inhibitörü kullanarak tersine çevirebildik. Ayrıca, Nek2A KO hücrelerinde Nusap1'in ubikitinasyonunda dikkate değer bir azalma gözlemledik. Bu durumun proteazomal bozulma süreçlerinin rolünü işaret ettiğini hipotezledik. Ayrıca, Nek2A knock out hücrelerde Nusap1 dahil birçok proteini içeren geniş bir protein analizi, azalan ifadelerini doğruladı.

Özetle, bulgularımız Nusap1'i yeni bir Nek2A partneri olarak işaret etti ve Nek2A'nın olası olarak Nusap1'in ubikitinasyon yoluyla parçalanmasını etkileyebileceğini düşündürdü. Bu etkileşimin tam doğası ve klinik önemidaha fazla araştırmalar yapılarak aydınlatılacaktır.

AKNOWLEDGEMENTS

I would like to express my heartfelt gratitude to Professor Ceyda Açılan Ayhan for her invaluable contributions to the completion of my thesis. During my time as a Master's student, her guidance and insights were among the most influential factors contributing to the achievement of my thesis objectives.

Furthermore, I want to extend my gratitude to Dr. Can Ozcan, who played a significant role as my advisor and research collaborator throughout my Master's research. His extensive expertise in the subject matter and hands-on experience with experiments were crucial in enriching my learning experience. I am genuinely thankful for his dedication to my academic growth, and his mentorship played an instrumental role in shaping my research journey.

I would also like to express my sincere appreciation to my friends, colleagues, and most importantly, my family, for their unwavering support throughout my Master's education. The encouragement and assistance I received from friends and colleagues during this academic journey were truly invaluable. I hold a special sense of gratitude for my family, as both their emotional and practical support played an immensely crucial role in my academic success. Their unwavering belief in my abilities and their willingness to support me through the challenges of my Master's education served as a constant source of motivation.

TABLE OF CONTENTS

LIST OF TABLES

LIST OF FIGURES

ABBREVIATIONS

KO	Knock out
DTB	Double Thymidine block
PCM	Pericentriolar material
LC-MS	Liquid chromatography–mass spectrometry
IP	Immunoprecipitation
PFA	Paraformaldehyde
EV	Empty Vector
WT	Wild Type
KD	Kinase Dead
KEGG	Kyoto Encyclopaedia of Genes and Genomes
CHX	Cycloheximide
GO	Gene Ontology

Chapter 1:
INTRODUCTION

1.1 Centrosomes

The centrosome is an organelle that lacks a membrane and functions as a microtubule organizing center. Centrosomes play a crucial role in various cellular functions such as cell division, cell motility, cellular transportation, and cell polarity. The size of centrosomes varies around 1μm, and consists of two centrioles, which are cylindrical structures with a diameter around 250nm and length varying from 150 to 500nm (Winey & O'Toole, 2014). The cylindrical structure of a centriole is the result of the formation of nine triplet microtubules (Schatten, 2008). γ-tubulin is required for the formation of the triplet structure of centrioles due to its microtubule nucleation function. Microtubule nucleation is the process of forming a microtubule seed through the polymerization of tubulin dimers. Nucleation via γ-tubulin induced scaffold is essential for cellular division (Job et al, 2003).

During cell division, the centrosome localizes into spindle poles through a series of complex processes. Centrosomes are duplicated by a controlled process, where each centriole grows one centriole from its side, and duplication occurs only once during the cell cycle, controlling the centrosome number in the cell (Nigg & Stearns, 2011). PLK4 is a key protein that initiates centriole assembly, and its down-regulation results in the inability of centrioles to duplicate, while its up-regulation leads to the over-duplication of centrosomes, resulting in extra centrosomes in the cell. PLK4 is also reported to induce de-novo production of centrioles, forming the cartwheel structure, which is the basis of the nine-triplicated structure. Centrioles are then elongated from the cartwheel structure to form mature structures, and the mother and daughter centrioles are separated from each other only to be linked via their proximal end via Cnap1 protein. The site of this connection forms the pericentriolar material (PCM). During the late S phase of the cell cycle, mother and daughter centrioles are separated and translocated to each pole of the cells (Fu et al, 2015).

Centrosome duplication and their localization to the spindle poles are crucial for proper bipolar spindle assembly. The accurate segregation of chromosomes during cell

division requires proper centrosome duplication, as duplicated chromosomes arrange themselves into a bipolar mitotic spindle assembly that pulls the chromosomes apart.

At early phase of the cell division, nuclear envelope breaks down, which allows the spindles to connect kinetochores (Silkworth et al., 2012). Kinetochores are connected to spindles via dynamic spindle microtubules (Cheerambathur et al., 2019). Any alterations in the centrosome duplication process, which could result in amplified centrosomes might affect the bipolar spindle formation. Non-bipolar spindle formation may result in chromosome segregation errors due to multiple spindle poles. This type of instability caused by centrosome amplification is a common property of some cancer cells. Cancer cells often have extra centrosomes, which contribute to chromosomal instability and aneuploidy (abnormal number of chromosomes), both of which are hallmarks of cancer. Therefore, understanding the regulation of centrosome duplication due to its impact on spindle poles and chromosome segregation is important for identifying potential targets for cancer treatment (Fukasawa, 2005).

Formation of multiple spindle poles makes cells highly unstable, typically leading to the induction of apoptosis and subsequent cell death. On the other hand, in many cases, cancer cells can avoid apoptosis despite the presence of extra centrosomes. This avoidance is often sustained by the clustering of centrosomes, even when there are more than two within the cell. Through clustering, the multiple centrosomes can form only two spindle poles, allowing the cancer cell to continue dividing without undergoing apoptosis. Expression of genes involved in centrosome clustering can have a synergistic effect on cancer cell viability, allowing these cells to continue to proliferate and contribute to tumor growth. Targeting these genes and disrupting centrosome clustering could be a promising therapeutic approach to induce apoptosis in cancer cells and inhibit tumor growth (Mittal et al., 2020) (Proteins Required for Centrosome Clustering in Cancer Cells, 2023).

Studies have shown an increase in the number of centrosomes in many types of cancer, such as brain, breast, gallbladder, colon, lung, pancreas, and prostate cancer (Nigg, 2002). The reasons behind this increase in number are attributed to three models: (i) excessive duplication, (ii) cell division transitioning to G1 phase before completion of mitosis (mitotic escape or aborted division), and (iii) cell fusions (Nigg, 2002). Although excessive centrosome pairing is generally achieved with DNA replication inhibitors such as hydroxyurea and aphidicolin, recent studies have shown that

overexpression of proteins responsible for centriole biogenesis can also cause centrosome amplification. Overexpression of PLK4 and STIL proteins, in particular, has been characterized in various cancer tissues with centrosome amplifications (Cosenza et al., 2017; Kleylein-Sohn et al., 2007; Ohta et al., 2018)

1.2 Nek2

Nek2A is a member of the serine/threonine protein kinase family and like many kinases, has numerous identified phosphorylation targets within cells (Fang and Zhang, 2016; Marina and Saavedra, 2014). Among these, the best-characterized targets are the centrosomal cohesion proteins known as C-Nap1, Rootletin, and Cep68, which are centrosome linking proteins. It has been shown that Nek2A localizes to the centrosome and phosphorylates these proteins, and that this phosphorylation is necessary for the separation of centrosomes during cell division (Bahe et al., 2005; Fry et al., 1998a; Man et al., 2015). The localization of Nek2A to the centrosome is regulated by the direct interaction between Nek2A and MST2, which is phosphorylated by PLK1 (Mardin et al., 2011). Moreover, Nek2A has been shown to contribute to the regulation of chromosome alignment through its direct interaction with MAD1 (Lou et al., 2004). In a study examining the effects of Nek2A on cell division, TRF1 was identified as a chromosomal target of Nek2A, and overexpression of Nek2A was found to result in centrosome amplification and aneuploidy in MDA-MB-231 and MCF7 cells (Lee and Gollahon, 2013a). In a different study, suppression of Nek2 by siRNA or chemical inhibition was found to result in an increase in centrosome number and cell division defects (Roberts et al., 2020). An increase in centrosome number can occur through various mechanisms and in different ways (e.g. increase in the number of centrioles, fragmentation of pericentriolar material, mitotic escape, cell fusion, etc.).

Nek2 is known to be a regulatory element for centrosome separation and chromosome segregation. Ensured distribution of genetic material during cell division by Nek2 protects cell from aneuploidy and consequently cancer progression. Nek2 levels are also elevated in cancer cells and known to function in tumour progression, and drug resistance. Another aspect of Nek2 activity is its suppression of a tumour suppressor gene p53 by phosphorylation (Carolina et al., 2021) (Choi et al., 2018).

1.3 TurboID proximity labelling

Proximity labeling analysis is a relatively new method that involves expressing the protein of interest as a fusion protein with a biotin ligase or ascorbate peroxidase enzyme and labeling the biotinylated proteins around this protein for identification. The BioID method was first used for this purpose, where a target protein linked to a biotin ligase with an R118G mutation (BirA*) is used, and biotin is applied to synthesize biotinoyl-5'-adenosine monophosphate (AMP) with enzymatic activity. This highly active biotin covalently binds to the accessible lysine residues of the surrounding proteins (Trinkle-Mulcahy, 2019). The biotinylated proteins can then be enriched with streptavidin and identified with LC-MS/MS. This method has been successfully used in centrosome biology (Firat-Karalar et al., 2014; Gupta et al., 2015) so far. APEX is a 27 kDa monomeric ascorbate peroxidase enzyme that catalyzes the oxidation of biotin-phenol in the presence of H_2O_2 to produce a short-lived (<1ms) intermediate compound, biotin-phenoxyl. This active biotin form also covalently binds to amino acids, such as tyrosine, tryptophan, cysteine, and histidine, which are rich in electron content (Beganton et al., 2019). APEX2 is an enzyme that has been catalytically activated to be more active than APEX (Lam et al., 2015). The advantages of the APEX method over the BioID method are that APEX has a smaller protein size (27 kDa for APEX, 35 kDa for BioID) and a shorter labeling time (1-5 minutes for APEX, 18-24 hours for BioID). However, H_2O_2 used in APEX methods can cause toxic effects on cells, so the BioID method has been developed to obtain the TurboID method (35 kDa), which can be labeled with a modified biotin ligase within 10 minutes (Trinkle-Mulcahy, 2019).

1.4 Mass Spectrometry

After the biotinylation of surrounding proteins with appropriate proximity labelling method, content of the biotinylated proteins should be analysed. Mass spectrometry methods are suitable for the detection of a given protein sample. LC-MS/MS, which stands for Liquid chromatography-tandem mass spectrometry, is a technique used to identify proteins in a sample based on their mass to charge ratio. The method involves converting the proteins into gas-phase ions, which can then be separated according to their mass to charge ratio. A detector is then used to identify the mass and charge of each ion (Han et al., 2008). Tandem mass spectrometry is a specialized technique that

involves fragmenting the proteins and analyzing the sequence of peptides using two mass analyzers. By utilizing liquid chromatography before tandem mass spectrometry, the speed and resolution of protein identification can be significantly increased. It is worth noting that LC-MS/MS is a powerful tool in proteomics research as it can identify a large number of proteins in a single sample, making it particularly useful in biomarker discovery and drug development. Additionally, advancements in LC-MS/MS technology have led to improved sensitivity, specificity, and accuracy in protein identification, making it an indispensable tool in modern life science research (Neagu et al., 2022)

Chapter 2:
METHODS

2.1 Cell Culture and Cell Cycle Synchronization and biotinylation.

All media was purchased from Sigma. Cells were grown in Dulbecco's modified Eagle's medium (DMEM) high glucose (cat: D5796), with 10% fetal bovine serum (FPS), Pen-strep at 37°C , 5% CO2. Doxycycline induction were made with 2 µg/mL. Cells were synchronized with double thymidine block. Cells were treated with 2.5 mM thymidine (cat: t9250-5g) for 18 hours, released by washing with PBS and fresh medium was added for 8 hours, and treated again with 2.5 mM thymidine for 18 hours. For the 0 h group cells were treated with 500 µM d-biotin (cat: B1595) for 30 minutes right before the end of second synchronization. For 5 h and 10 h groups cells were released by washing with PBS and fresh medium was added. 5 h group was treated with biotin at the 4.5 hour point of the third release for 30 minutes. 10 h group was treated with biotin at the 9.5 hour point of the third release for 30 minutes. All three groups were washed with cold PBS to stop biotinylation before pellet collection.

Overnight 20 µM STLC treatment then mitotic shake was used to collect cells at M stage of cell cycle.

2.2 Flow cytometry and Cell cycle assays

Cells were collected with trypsin after the synchronizations, fixed with 70% ethanol for overnight. Cells were relieved from ethanol with centrifuging at 4°C. Pellets than dissolved with RNAse1 for 10 minutes. Cells were incubated with propodium iodine for 30 minutes. PI and Rnase1 is removed by centrifuge and cell were subjected to flow cytometry. Results were analysed and visualised with FlowJo

2.3 Cloning

mRNAs were purified from U2OS cell lines, converted to cDNA and amplified with PCR to obtain Nusap1 cDNA. Amplified product than cloned to pLJC2-GPT2-3XFLAG plasmid. HEK293T cells were transfected with Nusap1 3xFLAG plasmid for viral packaging. Viruses were collected from medium at second and third day of transfection. Collected mediums were filtered with 0.40 µm filters and mixed with PEG

(cat: 043443.A9). After 2 days tubes were centrifuged and PEG bound virus pellets were dissolved with PBS. U2OS and U2OS Nek2 KO B9 cells were transduced with obtained viruses. Cells were selected with 1.5 μg/mL Puromycin after a day from virus treatment for two days.

2.4 Biotin Affinity Purifications

Cells were lysed with Ripa buffer (0.1% NP-40 (cat: PI28324), 0.05% Sodium deoxycholate (cat: 89904), 0.01% SDS (cat: 1610418), 15 mM NaCl (cat: 7647-14-5), 5 mM, pH 8.0 Tris-Cl (17926), Protease inh (cat: A32965), Phosphatase inh (cat: 05892791001), PMSF (cat: P7626)). Centrifuged at 15000g for 15 minutes to remove cell debris. BCA assay was used for the quantification of protein concentration. Proteins for each samples were incubated with resin-streptavidin beads for overnight at 4°C. After the treatment beads were washed for 4 times. For western blot samples method at "western blot" section was used. For the Mass Spec samples "LC-MS" analysis section was used.

2.5 LC-MS analysis

C18 nanoflow reversed-phase HPLC (Dionex Ultimate 3000,3500 RSLC nano, Thermo Scientific) and orbitrap mass spectrometer (Q Exactive Orbitrap, Thermo Scientific) combination were used for peptide analysis. Samples were run with 300 nl/min flow for 60 min in 4-25%, 25-45%, 45-95% acetonitrile in 0.1% formic acid. 70000 resolution (AGC 3e6) Max IT 60 ms with Scan range 400-1500 m/z with MS1 scan and 17 500 resolution (AGC:5e4) Max IT:60 ms with MS2 scan. Top 15 ions were fragmented and analysed in an isolation window of 2.0 m/z. (Ozkan et al, 2023).

MaxQuant was used for analysis of thermo raw files. LFQ analysis performed with match between runs were selected. Results were further analysed with Cassiopeia_LFQ (WeiqiangChen, 2023).

Amica tool was utilized for analysis as well (Didusch et al, 2022).

Raw data accession number: PXD046115

2.6 Immunoprecipitations

,Cells were collected by trypsinization (0.05%). Pellets were treated with 1% PFA (cat: 104005.1000)for 7 minutes. After PFA fixation cells were centrifuged to remove PFA and quenched with 1.25mM ice cold glycine. Glycine was removed by centrifuge. For non-PFA immunoprecipitation cells were lysed directly. Cells were lysed with IP buffer (cat: 87787), supplemented with protease inhibitor, phosphatase inhibitor, and PMSF at ice for 45 minutes. BCA assay was used for quantification of protein concentration. Protein G Magnetic Beads (cat: 1004D) were incubated with cell lysates for pre clearance for 30 minutes. Magnetic beads were removed and protein samples were incubated with either FLAG antibody(cat: F3040) or IGG (cat: sc-2025) for 2 hours at 4C. After two hours antibody-protein mixture was incubated with protein G magnetic beads for overnight. After the incubation, beads were washed four times and beads were denaturated with 4x laemli buffer (cat: 1610747) with 10% DTT (20290) for 15min at 95°C. Western blot procedure is used for blotting. For ubiquitination experiments cells were treated with 10 μM MG132 for 5 hours prior to immunoprecipitation.

2.7 Western Blot

Cells were lysed with Ripa buffer (0.1% NP-40, 0.05% Sodium deoxycholate, 0.01% SDS, 15 mM NaCl, 5 mM, pH 8.0Tris-Cl, Protease inh, Phosphatase inh, PMSF) at ice for 15 minutes. Centrifuged at 15000g for 15 minutes to remove cell debris. Thermo BCA assay was used for the quantification of protein concentration. Lysates were denatured with 4x laemli buffer with 5% DTT for 12min at 95°C. 4% to 15% gradient SDS-PAGE gels were used. 5% non-fat-dry milk (brand) in 1xTBST was used for 1 hour blocking at RT. Primary antibodies were incubated overnight at 4°C. Membrane were incubated with secondary antibodies (1:5000) at RT for 1 hour. Blots were visualised with Forte (brand) at (imaging system brand)

2.8 Immunofluorescence Microscopy

Cells on the coverslips were fixed with -20°C methanol or RT 4% PFA for 10 minutes. PFA fixed cells were treated with 0.2% Triton X-100 for 10 minutes. After the fixation coverslips were blocked with 5% BSA (Sigma; 9048) in PBS at RT, then

incubated with primary antibodies for overnight at 4°C. Cover slips were washed and incubated with secondary antibodies for one hour. Mounted at slides with DAPI mounting medium (Vectashield). Imaging was done with fluorescent and confocal microscopy.

2.9 ELISA

For the enzyme-linked immunosorbent assay direct ELISA protocol by (Lin, 2015) was used. Proteins were coated to the 96 well plates with carbonate bicarbonate buffer for overnight at 4°C, denaturated with 2% SDS for 30 min, and blocked with SuperBlock Blocking Buffer (cat: 37515). After blocking plate is incubated with StreptavidinHRP (21140) and quantified after Pierce™ ECL Western Blotting Substrate (cat: 32109) induction.

2.10 Antibodies

Table 1 List of Antibodies with their Catalog number

Brand	Name	Cat no
BD bioscience	Nek2	610594
CST	Gapdh	mAb #2118
CST	Alpha Tub	mAb #2125
CST	Beta Actin	mAb #3700
Sigma	γ Tub	T6557
Santa Cruz	Cycline	sc-247
Santa Cruz	Kif2c	sc-81305
Ab Clonal	Nusap1	A16000
Ab Clonal	Mapre3	A19768
Ab Clonal	Mpg	A18070
Ab Clonal	Rab6	A5613
Ab Clonal	Dek	A0315
Ab Clonal	Taok1	A21157
Ab Clonal	Cenpf	A18644
Ab Clonal	Smurf2	A2278
Ab Clonal	Ckap4	A7777
Ab Clonal	Nsun4	A14983
Ab Clonal	Mark3	A19324
Ab Clonal	Kifc1	A16548
Ab Clonal	Plk1	A21082
Protein Tech	Kif2a	13105-1-AP
Protein Tech	Kif20a	15911-1-AP
Sigma	FLAG	F3040

Chapter 3:
RESULTS

3.1 TurboID fused Nek2 constructs are dox inducible and stable.

TurboID functions as a biotin ligase, facilitating the biotinylation of target proteins situated in close proximity to the bait protein. To introduce Nek2WT and Nek2KD fused TurboID constructs into U2OS cell lines, a tet-on promoter system was employed. The induction of transcription for these constructs was achieved through the administration of 2 µg/mL doxycycline over a span of two days. Subsequent Western blot analyses utilizing both FLAG and Nek2 antibodies corroborated the successful translation of TurboID, TurboID-Nek2WT, and TurboID-Nek2KD proteins, while also affirming their sustained presence within the cellular environment.

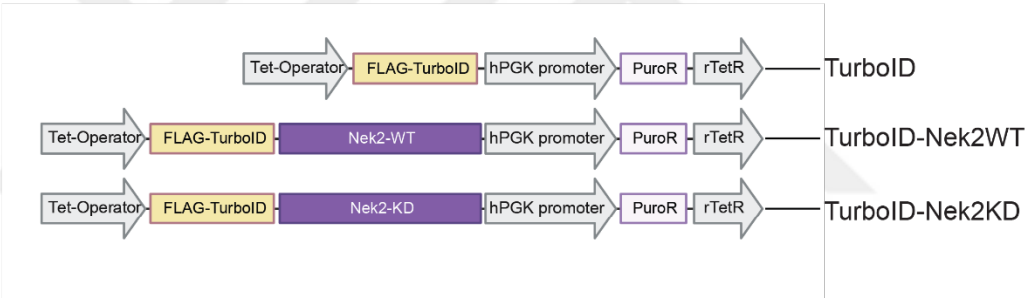

Figure 3-1 TurboID constructs are doxycycline inducible, FLAG tagged lentiviral constructs

Generated by Dr. Selahattin Can Ozcan

It is worth noting that, in an intriguing observation, even though both TurboID-Nek2WT and TurboID-Nek2KD proteins carry a FLAG tag analogous to that of the TurboID empty vector, the anti-FLAG antibody exhibited an inability to detect the Nek2-fused proteins. Nevertheless, the anti-Nek2 antibody demonstrated its efficacy in confirming the successful overexpression of TurboID-Nek2WT and TurboID-Nek2KD. This different response of antibodies indicates the complexity of protein interactions and antibody specificity.

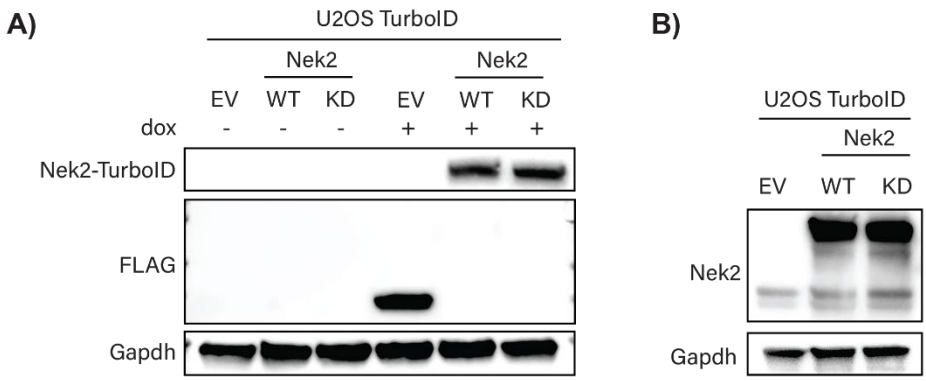

Figure 3-2 Western blot confirmation of dox induced TurboID protins

A) After two days of doxycycline induction cell lysates were subjected to western blotting with anti-FLAG and Anti-Nek2 antibodies. Cells successfully expressed the TurboID constructs with dox induction.

B) Endogenous Nek2 proteins expression is present at the engineered cells after dox induction of TurboID-Nek2 proteins.
Anti-Gapdh blot is used as a loading control.

3.2 TurboID fused Nek2 constructs localizes primarily to centrosomes as endogenous Nek2A.

To ascertain the subcellular localization of the engineered TurboID constructs, a series of immunofluorescence experiments were conducted. Following a two-day period of doxycycline induction, cells were fixed utilizing methanol as a fixative agent. Through the utilization of confocal microscopy coupled with antibodies targeting both the FLAG epitope and gamma tubulin, it was revealed that the TurboID-Nek2WT and TurboID-Nek2KD fusion proteins exhibited a distinct localization pattern, specifically at the centrosomes. In contrast, the only TurboID-containing empty vector (EV) proteins displayed a more diffuse distribution throughout the cellular landscape. This divergence in localization patterns indicated that the presence of Nek2 proteins was sufficient to guide their correct transportation to their native subcellular localization, despite the TurboID presence.

Furthermore, the dispersed localization of the EV-TurboID proteins rendered them well-suited for utilization as a control in subsequent biotinylation experiments. The absence of concentrated localization in this context corresponds to a more widespread distribution of biotinylation potential. In essence, the pattern of localization observed in the immunofluorescence analysis was corroborated by the subsequent biotinylation outcomes, further strengthening the relationship between protein localization and the ensuing biotinylation activity.

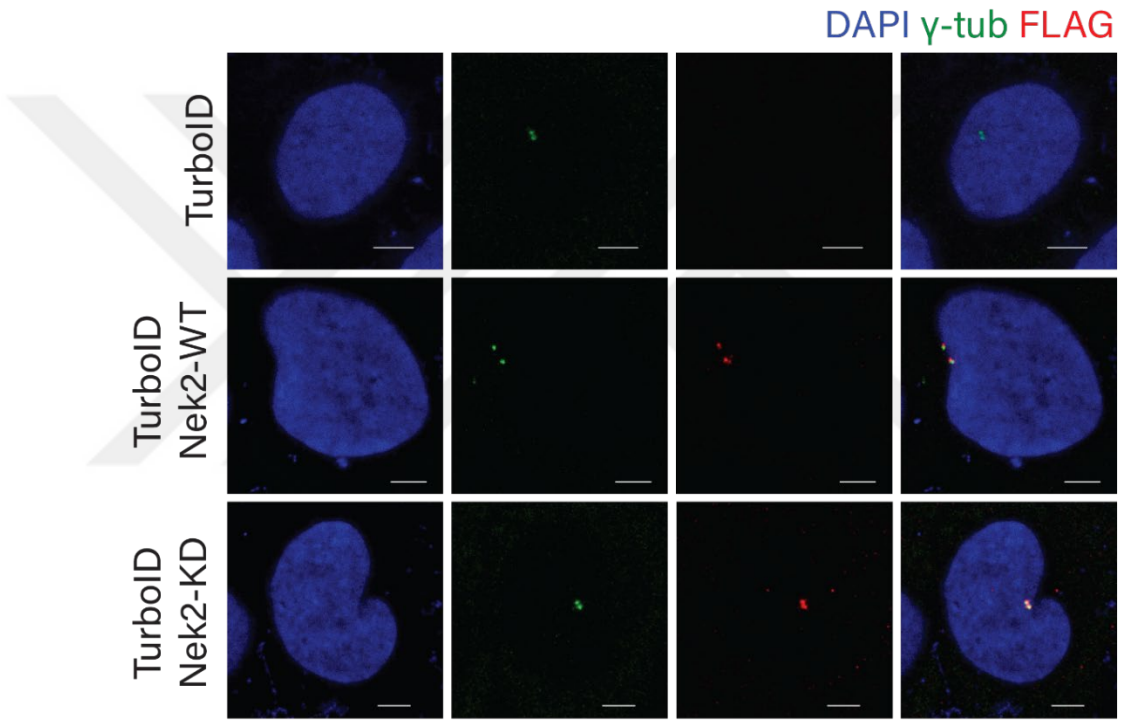

Figure 3-3 Immunofluorescent imaging with anti-FLAG and anti-gamma tubulin antibodies validates the centrosomal localization of TurboID-Nek2WT and TurboID-Nek2KD proteins. TurboID proteins are fused with FLAG tag. Gamma tubulin was used as a centrosomal marker.

3.3 Overexpression of TurboID fused Nek2 constructs are not exhibiting unintended separation of the centrosomes and Nek2 overexpression does not affect cell cycle flow.

A significant concern when employing engineered proteins for proximity labeling is the potential for unintended activities arising from their overexpression. In the context of this study, Nek2, which is recognized for its role in mediating the separation of centrosomes by disrupting the linkage between centrioles, was selected for investigation. The objective was to assess whether the overexpression of Nek2 might lead to premature or incomplete separation of centrosomes, thereby indicating unintended functional alterations.

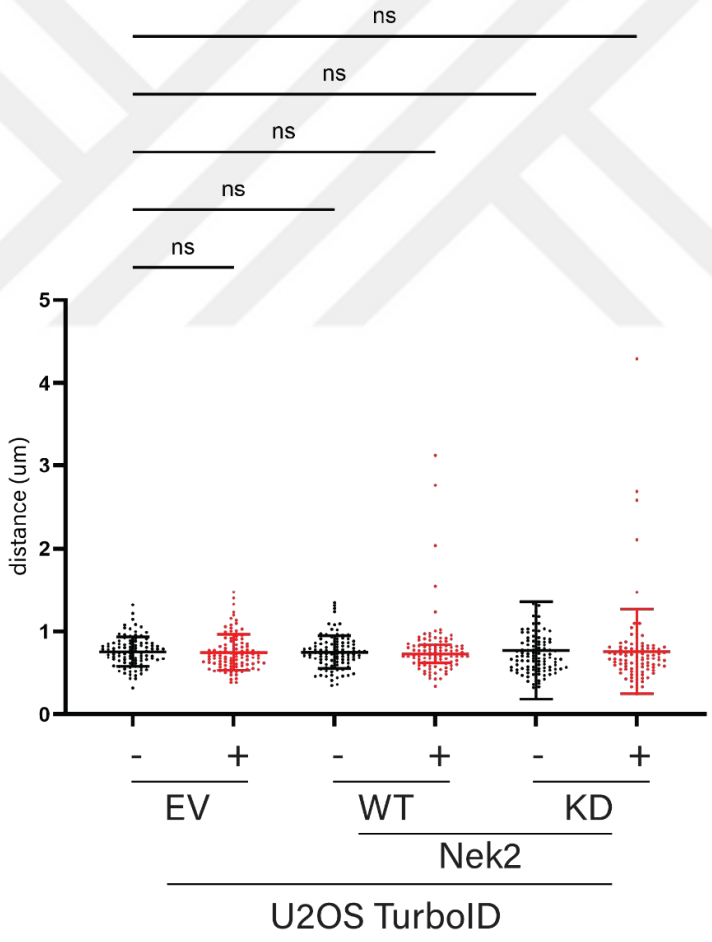

Figure 3-4 Distance between centrosome are quantified after two days of dox induction via immunofluorescent experiment.

There is no significant unintended separation of centrosome due to Nek2 overexpression with TurboID.

To evaluate this, an immunofluorescence experiment was conducted utilizing an anti-gamma tubulin antibody. The approach involved quantifying the distance between centrosomes within a pool of one hundred cells, both in the presence and absence of doxycycline induction. Despite observing a limited number of cells that exhibited a noticeable increase in the distance upon Nek2 overexpression, statistical analysis revealed that these variations were not significant. Consequently, the data indicated that the overexpression of TurboID-fused Nek2 did not result in functional irregularities concerning the premature separation of centrosomes.

Another unintended effect of Nek2 overexpression could be over cell cycle progression. To evaluate possible effects of Nek2 overexpression, comparative cell cycle analysis of Nek2 overexpression and its negative controlled were performed by flow cytometry. After two days of doxycycline (2 µg/ml) induction, cells were fixed with 70% ethanol and stained with propidium iodide. Comparison of two groups revealed there is no significant difference arises from Nek2 overexpression.

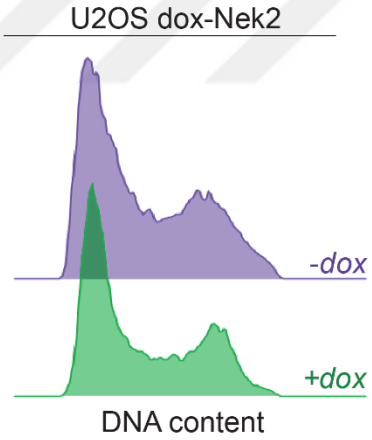

	-dox	+dox
G1	51.8	54.8
S	24.1	24.9
G2	22.6	19.5

Figure 3-5 Cell cycle analysis of Nek2 overexpressing cells with flow cytometry

Nek2 overexpression is triggered with two days of doxycycline induction. Then cells were collected and fixed with 70% ethanol. After RNAse and Propidium iodide incubation cells were subjected to flow cytometry analysis.

3.4 TurboID successfully performs its biotin ligase activity

Following a two-day period of doxycycline-induced TurboID expression, biotinylation was initiated through a 30-minute exposure to 500 μM biotin. Subsequent Western blot analysis employing Streptavidin-HRP indicated the successful execution of biotin ligase activity across the experimental groups: EV-TurboID, TurboID-Nek2WT, and TurboID-Nek2KD. An intriguing observation emerged, as the biotinylation activity induced by EV-TurboID was notably higher in comparison to the biotinylation activity observed in the Nek2-fused TurboID constructs.

To quantitatively ascertain the distinctions in biotinylation levels across the diverse experimental groups, a direct enzyme-linked immunosorbent assay (ELISA) methodology was employed. In this approach, protein extracts obtained from TurboID-expressing cells treated with doxycycline and biotin were immobilized onto a 96-well plate. Subsequent application of Streptavidin-HRP enabled the detection of biotinylated proteins. The outcomes of the ELISA experiment unveiled a substantial difference, with EV-TurboID expressing cells demonstrating 6-7 times greater total biotinylated protein levels than their Nek2-fused counterparts when subjected to biotin treatment.

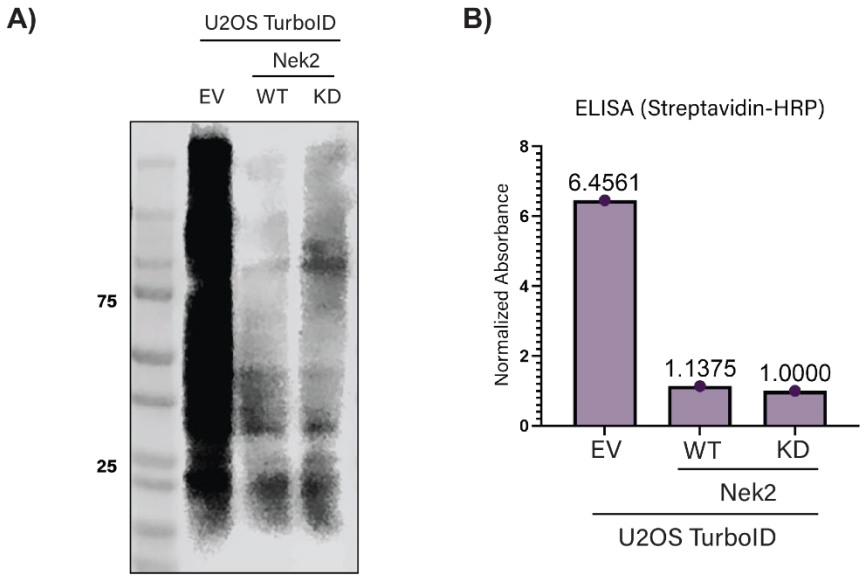

Figure 3-6 Total biotinylation by TurboID proteins.

A) TurboID constructs successfully performs their biotin ligase activity at 30 minutes. Streptavidin-HRP western blot show that EV-TurboID biotiniylates dramatically more than TurboID-Nek2WT and TurboID-Nek2KD

B) The quantitative total biotinylation difference between these three groups are examined with direct enzyme-linked immunosorbent assay (direct-ELISA) with Streptavidin-HRP andibody.

3.5 Close proximity proteins are successfully tagged with TurboID-mediated biotin labeling

U2OS cells stably expressing TurboID constructs underwent a two-day treatment with doxycycline, followed by a 30-minute biotinylation period using 500 μM d-biotin. The resultant protein extracts from these cells were subsequently subjected to an overnight incubation with streptavidin-coupled resin beads. The subsequent streptavidin pulldown procedure facilitated the enrichment of biotinylated proteins, which were then evaluated through Western blot analysis.

Employing both anti-FLAG and anti-Nek2 antibodies in the Western blot analysis, successful self-biotinylation of the TurboID constructs was evident. This was further substantiated by the successful pulldown of biotinylated proteins using streptavidin-resin beads. Notably, the previously observed challenge in detecting Nek2-fused TurboID proteins through FLAG antibody was circumvented after the streptavidin pulldown, enabling the detection of TurboID-Nek2WT and TurboID-Nek2KD proteins.

Of significance, the experiment shed light on the biotinylation of endogenous Nek2 proteins. TurboID-Nek2WT and TurboID-Nek2KD successfully biotinylated endogenous Nek2, a finding that holds dual implications. Firstly, the specificity of the experimental approach was validated, and secondly, the endogenous Nek2 is notable despite overexpressed TurboID-Nek2 proteins.

Furthermore, a Streptavidin-HRP blot was conducted post streptavidin pulldown. In this analysis, the enhanced biotinylation of TurboID-Nek2WT and TurboID-Nek2KD was more discernible. Nonetheless, a notable disparity persisted in the biotinylation contrast between EV-TurboID and TurboID-Nek2 cells. Interestingly, TurboID-Nek2 cells treated with doxycycline exhibited a substantially elevated level of biotinylation compared to untreated TurboID cells. Notably, while the biotinylation of Nek2 constructs remained relatively modest, it exceeded the levels of endogenous biotinylation, indicating the potency of the TurboID-mediated biotin labeling.

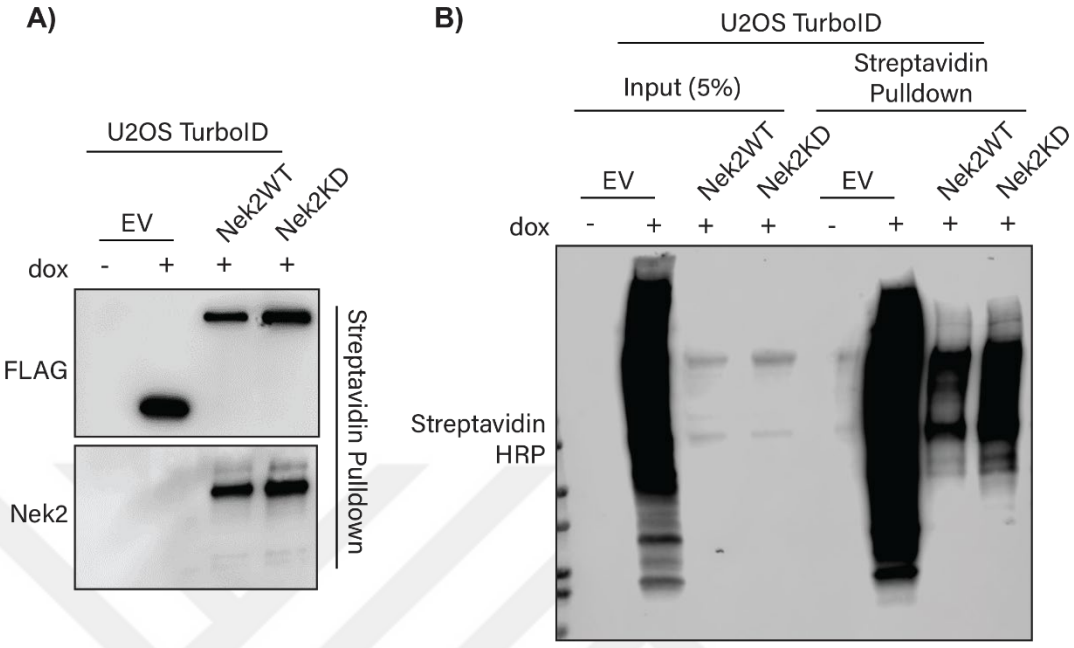

Figure 3-7 Biotinylated proteins are pulled down with streptavidin coated resin beads

A) Pull downed protein samples were subjected to western blotting with Anti-FLAG and anti-Nek2 antibodies. TurboID protein successfully biotinylated itself. TurboID-Nek2WT and TurboIDNek2-KD proteins biotinylated themselves and endogenous Nek2. Streptavidin pulldown successfully separated biotinylated proteins

B) Pull downed protein samples were subjected to western blotting with Streptavidin-HRP. Streptavidin pulldown enriched the biotinylated proteins surrounding TurboID-Nek2WT and TurboID-Nek2KD proteins

Blot by Dr. Can Ozcan

3.6 Biotinylation ligase activity of TurboID-Nek2 proteins mostly occurs around centrosome.

Immunofluorescence experiments involving Streptavidin-488 labeling were conducted to elucidate the spatial distribution of biotinylated proteins. The findings revealed that Nek2-fused constructs predominantly biotinylated proteins localized in the vicinity of centrosomes. Conversely, cells harboring EV-TurboID exhibited biotinylation distributed throughout the entirety of the cell. This contrast signifies that, upon comparison, enriched proteins in the Nek2 groups to EV-TurboID should primarily consist of centrosome-associated proteins. Furthermore, dispersed localization of the EV-TurboID protein potentially contributes to the increased biotinylation observed relative to the Nek2-fused constructs.

+dox -biotin group showed no localized biotinylation compared to +dox +biotin groups. Therefore, dialyzed FBS, which does not contain biotin, was reliable to inhibit unintended biotinylation by expressing constructs over two days. Biotin ligase activity of TurboID is only limited to 30 minutes interval of d-biotin incubation.

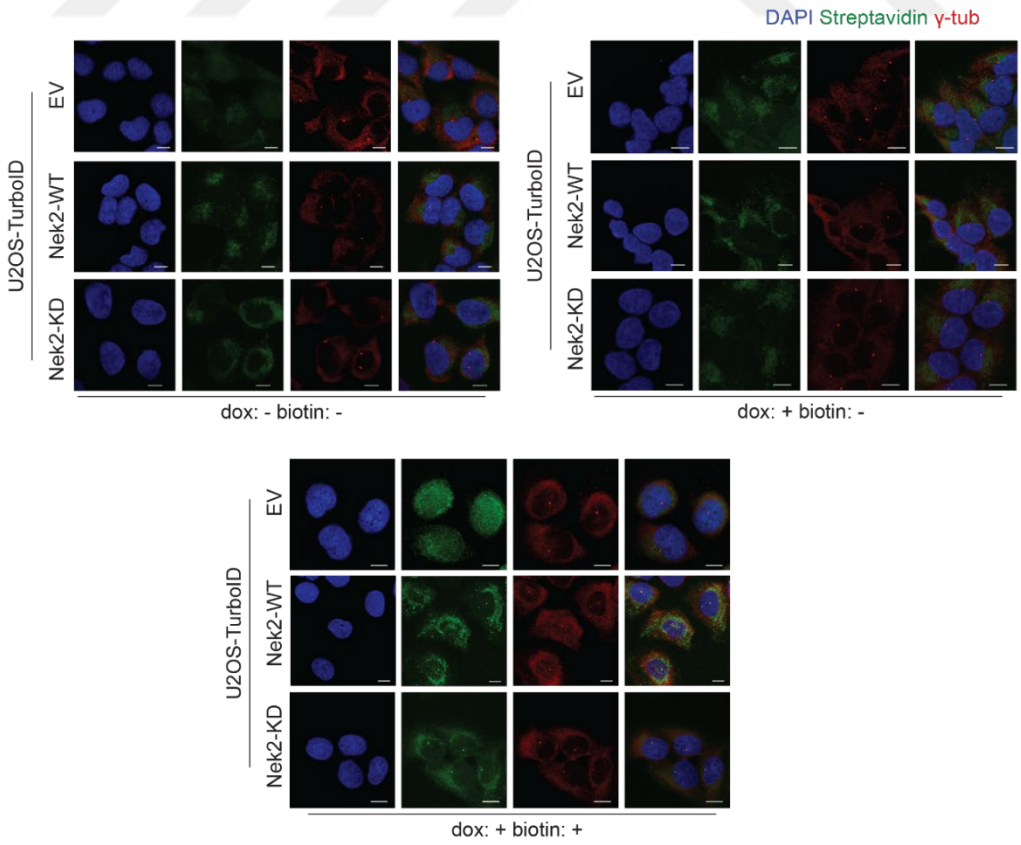

Figure 3-8 Centrosome localization of biotinylation is confirmed with immunofluorescent experiment with streptavidin-488 and anti-gamma tubulin

Cell were treated with or without doxycycline for two days and incubated with d-biotin for 30 minutes before methanol fixation. TuboID-Nek2WT and TurboID-Nek2KD proteins are mostly biotinylated centrosome while TurboID only control biotinylated over cell dispersedly.

3.7 Mass Spectrometry analysis of unsynchronized TurboID mediated proximity labelling

Following the confirmation of the successful translation of TurboID constructs and their subsequent biotinylation at expected target regions, a substantial number of cells were biotinylated and their protein content is isolated. These biotinylated proteins were isolated through an affinity purification process employing streptavidin-coated resin beads. The enriched proteins obtained from this pulldown were subjected to analysis via liquid chromatography-mass spectrometry (LC-MS).

The raw data originating from the Thermo MS instrumentation were subjected to analysis using the MaxQuant software. MaxQuant facilitated the comparative examination of different experimental groups, enabling the normalization of protein intensities across the groups. Following the MaxQuant analysis of the mass spectrometry data, notable disparities between the Nek2 groups and the TurboID-EV group became evident. These disparities manifested in terms of both protein quantities and their corresponding intensities, which exhibited substantial discrepancies. The extent of this dissimilarity posed a hindrance to the straightforward application of statistical analyses.

To mitigate the challenges posed by the substantial inter-group differences, an imputation methodology was employed. The Cassiopeia program was utilized for this purpose, resulting in the implementation of imputation strategies that rendered all experimental groups comparable without exerting undue influence on the subsequent analyses. Subsequent to the imputation process, statistical analysis was conducted using the limma framework.

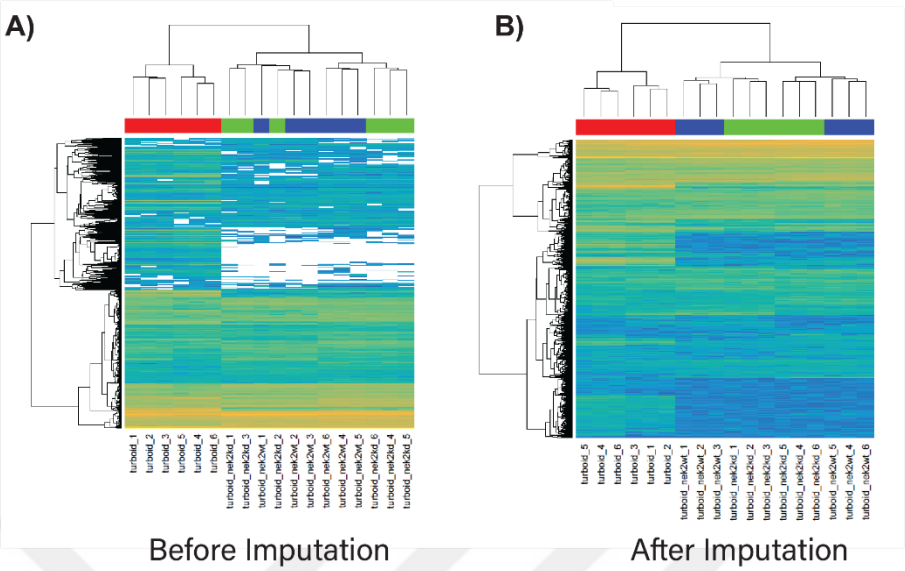

Figure 3-9 Normalized intensities of detected proteins before and after imputation.

A) Before the imputation substantial amount of proteins detected at TurboID control group were missing at Nek2WT and Nek2KD groups.

B) Imputation normalized the distribution of total proteins for a relevant statistical analysis.

with Dr S Can Ozcan

After the statistical analysis, significantly enriched proteins compared to control group were revealed. Among those proteins Nek2 was the highest in terms of fold change as expected. Other than Nek2, already known Nek2 targets, such as Kif24, anaphase promoting complex proteins were also identified. This indicated the success of the TurboID biotinylation and following pulldown. Total 700 proteins were enriched in both groups. 108 of these proteins were specific to TurboID-Nek2WT group, while 106

proteins only enriched at TurboID-Nek2KD. 466 proteins were enriched in both Nek2 groups.

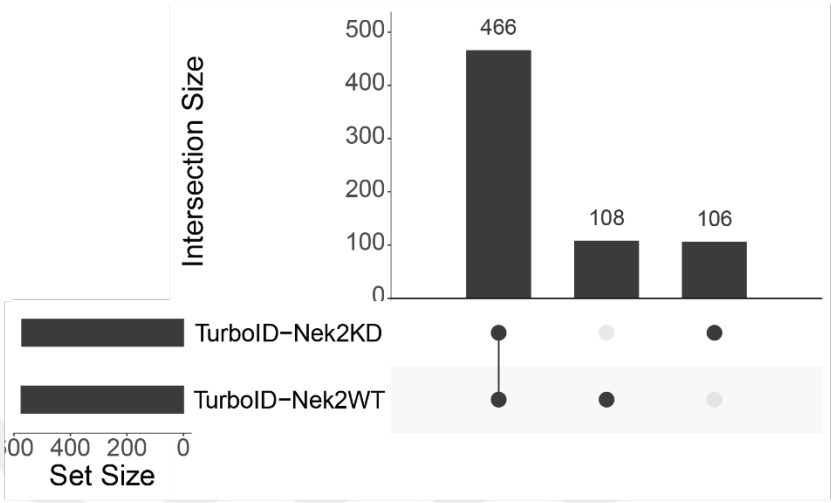

Figure 3-10 UpSet plot to compare number of specific and common enriched proteins at Nek2WT and Nek2KD groups.

Total 700 proteins were enriched in both groups. 108 of these proteins were specific to TurboID-Nek2WT group, while 106 proteins only enriched at TurboID-Nek2KD. 466 proteins were enriched in both groups.

Pathway analysis of positively enriched proteins of both groups reveals common pathways as substantial amount of proteins are commonly enriched. Some of the interesting pathways that are enriched with the lowest false discovery rate (FDR) value are; ribosome biogenesis in eukaryotes, cell cycle, base excision repair, and ubiquitin mediated proteolysis. Enrichment of cell cycle term was expected since Nek2 is a cell cycle regulated protein.

Cellular component analysis revealed that most of the proteins that were enriched were spindle pole, centrosome and microtubule related. Since Nek2 is centrosome localized protein, enrichment of spindle pole, centrosome and microtubule terms were expected. Other than microtubules, lamin complex and DNA replication complex was enriched, which suggested possible Nek2 activity in the nucleus. Kinetochore complex enrichment confirms the already known Nek2 activity at kinetochores.

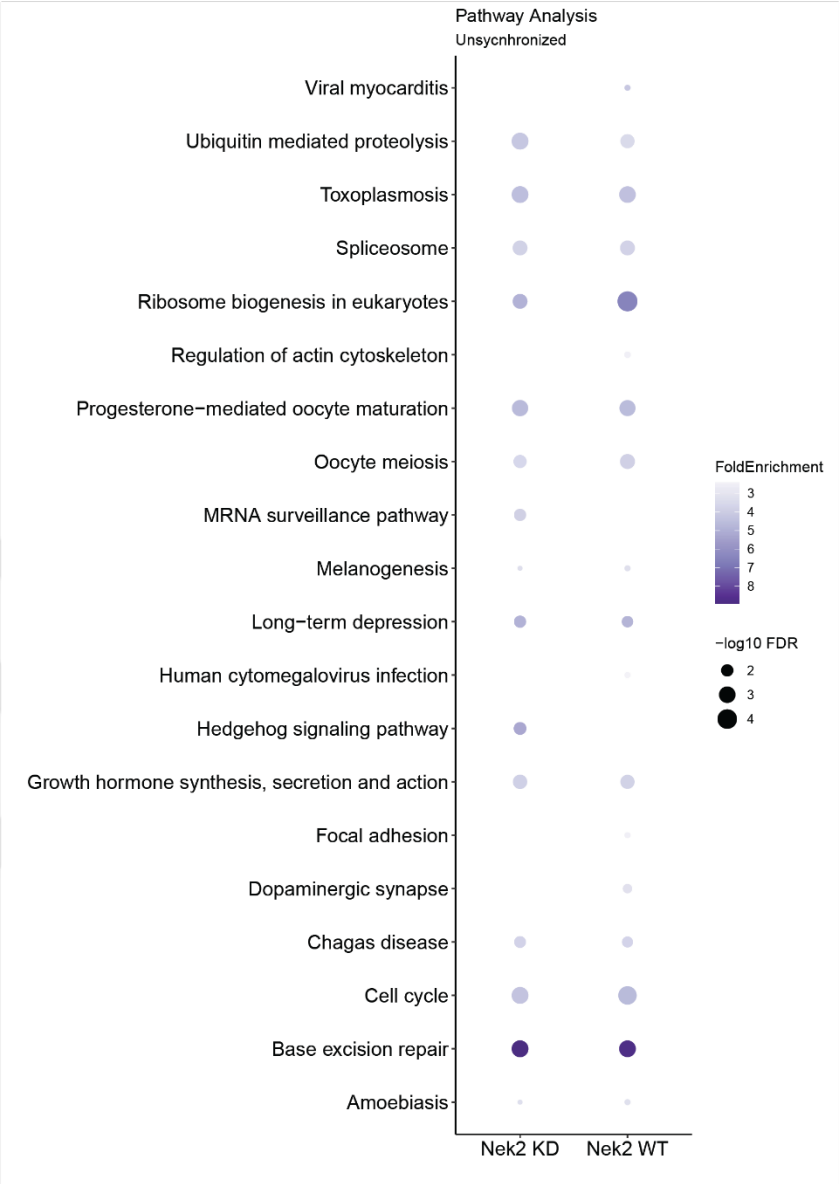

Figure 3-11 KEGG – Pathway analysis of positively enriched proteins of Nek2WT and Nek2KD groups.

Significantly enriched proteins were subjected to pathway analysis by shinygo online tool

Figure 3-12 Cellular component analysis of positively enriched proteins of Nek2WT and Nek2KD groups.

Significantly enriched proteins were subjected to pathway analysis by shinygo online tool. Pathways over 10 fold enrichment were visualised for both groups due to excessive quantity

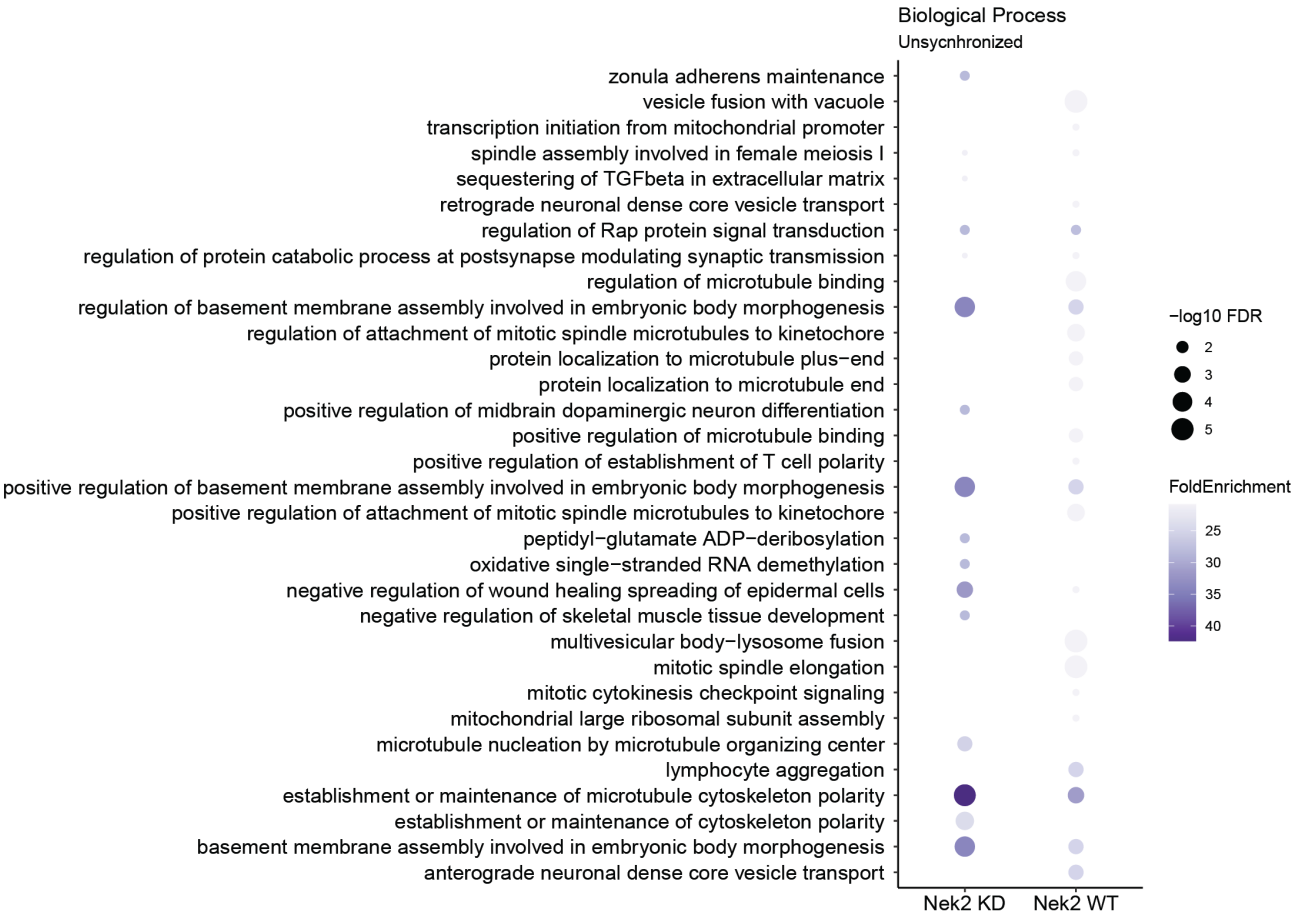

Figure 3-13 Biological process analysis of positively enriched proteins of Nek2WT and Nek2KD groups.

Significantly enriched proteins were subjected to pathway analysis by shinygo online tool. Pathways over 20 fold enrichment were visualised for both groups due to excessive quantity

Biological process analysis revealed that most of the proteins that are enriched are cytoskeleton polarity and regulation of microtubule binding related. Since Nek2 is known to be localized to the centrosome, enrichment of proteins that function at cytoskeleton polarity and microtubule binding was expected. Nevertheless, enrichment of membrane assembly involved in embryonic body morphogenesis, and regulation of Rap protein signal transduction is quite interesting and could reveal unknown functions of Nek2

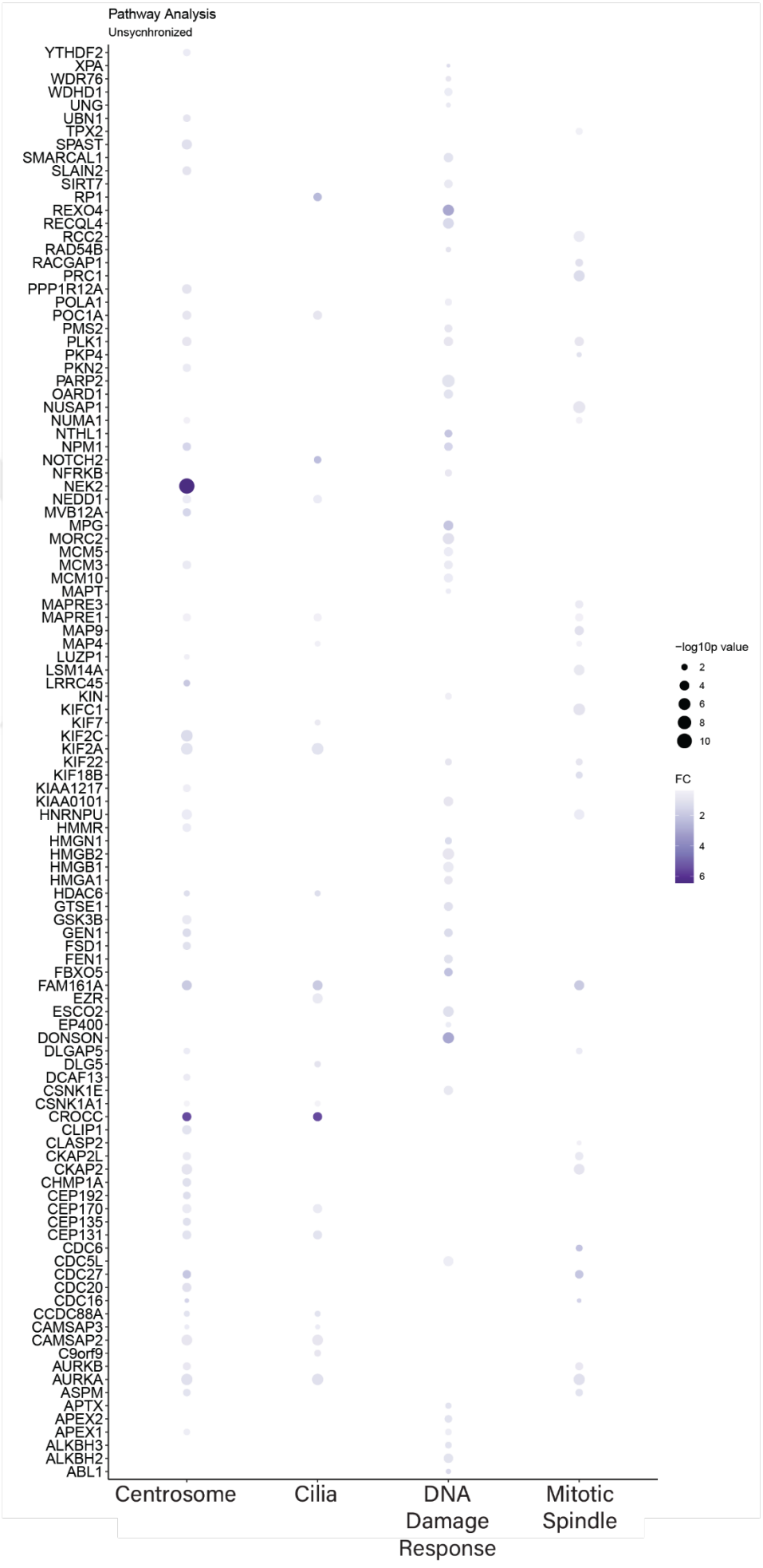
Pathway Analysis
Unsycnhronized
YTHDF2
XPA
WDR76
WDHD1
UNG
UBN1
TPX2
SPAST
SMARCAL1
SLAIN2
SIRT7
RP1
REXO4
RECQL4
RCC2
RAD54B
RACGAP1
PRC1
PPP1R12A
POLA1
POC1A
PMS2
PLK1
PKP4
PKN2
PARP2
OARD1
NUSAP1
NUMA1
NTHL1
NPM1
NOTCH2
NFRKB
NEK2
NEDD1
MVB12A
MPG
MORC2
MCM5
MCM3
MCM10
MAPT
MAPRE3
MAPRE1
MAP9
MAP4
LUZP1
LSM14A
LRRC45
KIN
KIFC1
KIF7
KIF2C
KIF2A
KIF22
KIF18B
KIAA1217
KIAA0101
HNRNPU
HMMR
HMGN1
HMGB2
HMGB1
HMGA1
HDAC6
GTSE1
GSK3B
GEN1
FSD1
FEN1
FBXO5
FAM161A
EZR
ESCO2
EP400
DONSON
DLGAP5
DLG5
DCAF13
CSNK1E
CSNK1A1
CROCC
CLIP1
CLASP2
CKAP2L
CKAP2
CHMP1A
CEP192
CEP170
CEP135
CEP131
CDC6
CDC5L
CDC27
CDC20
CDC16
CCDC88A
CAMSAP3
CAMSAP2
C9orf9
AURKB
AURKA
ASPM
APTX
APEX2
APEX1
ALKBH3
ALKBH2
ABL1
Centrosome
Cilia
DNA Damage Response
Mitotic Spindle
−log10p value
2
4
6
8
10
FC
2
4
6

Figure 3-14 Individual proteins that are significantly enriched in Nek2WT group that are a part of following GO-Terms; Centrosome, Cilia, DNA Damage Response, and Mitotic Spindle.

Enriched proteins of Nek2WT group were analysed by direct comparison to following GO-Terms; Centrosome, Cilia, DNA Damage Response, and Mitotic Spindle to find potential targets of Nek2. Even though DNA Damage Response is not a known Nek2 related function compared to Centrosome, Cilia, and Mitotic Spindle.

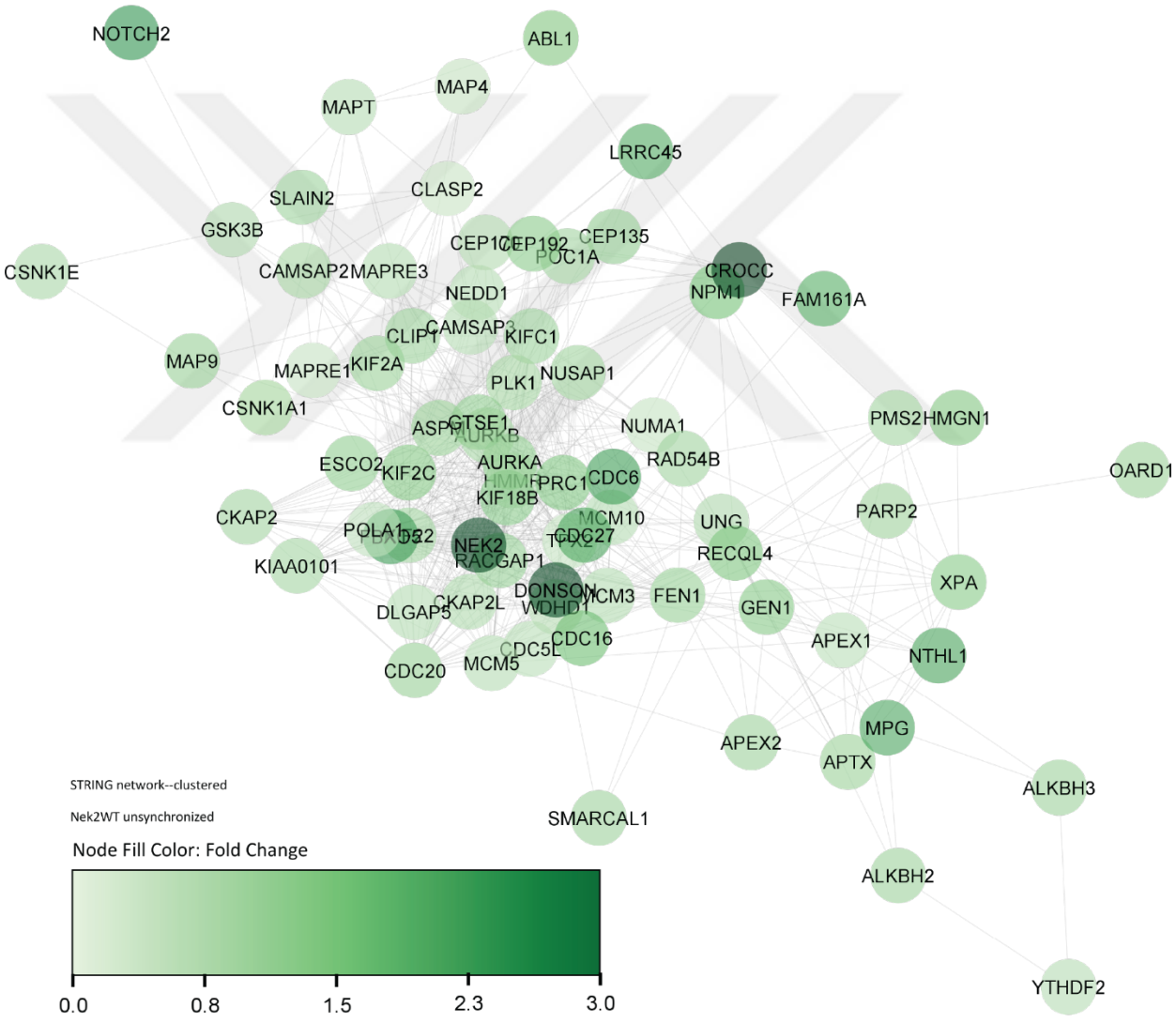

Figure 3-15 String analysis of proteins that are positively enriched at Nek2WT group which are also a part of Centrosome, Cilia, DNA Damage Response, and Mitotic Spindle GO terms in pathway analysis.

Proteins that are enriched in Nek2WT and are a part of Cilia, DNA Damage Response, and Mitotic Spindle GO-terms are analysed with string app at Cytoscape program. MCL clustering with 3 factor is applied and main cluster is coloured according to TurboID-Nek2WT fold change.

To visualise the potential targets, enriched proteins that are a part of Centrosome, Cilia, DNA Damage Response, and Mitotic Spindle GO-terms are analysed with Sting-Cytoscape and clustered with MCL clustering. String analysis with clustering revealed that most of those proteins are forming a single cluster and potentially associated with each other and Nek2. Nek2 is at the centre of this cluster, which also indicate the realibility of TurboID system.

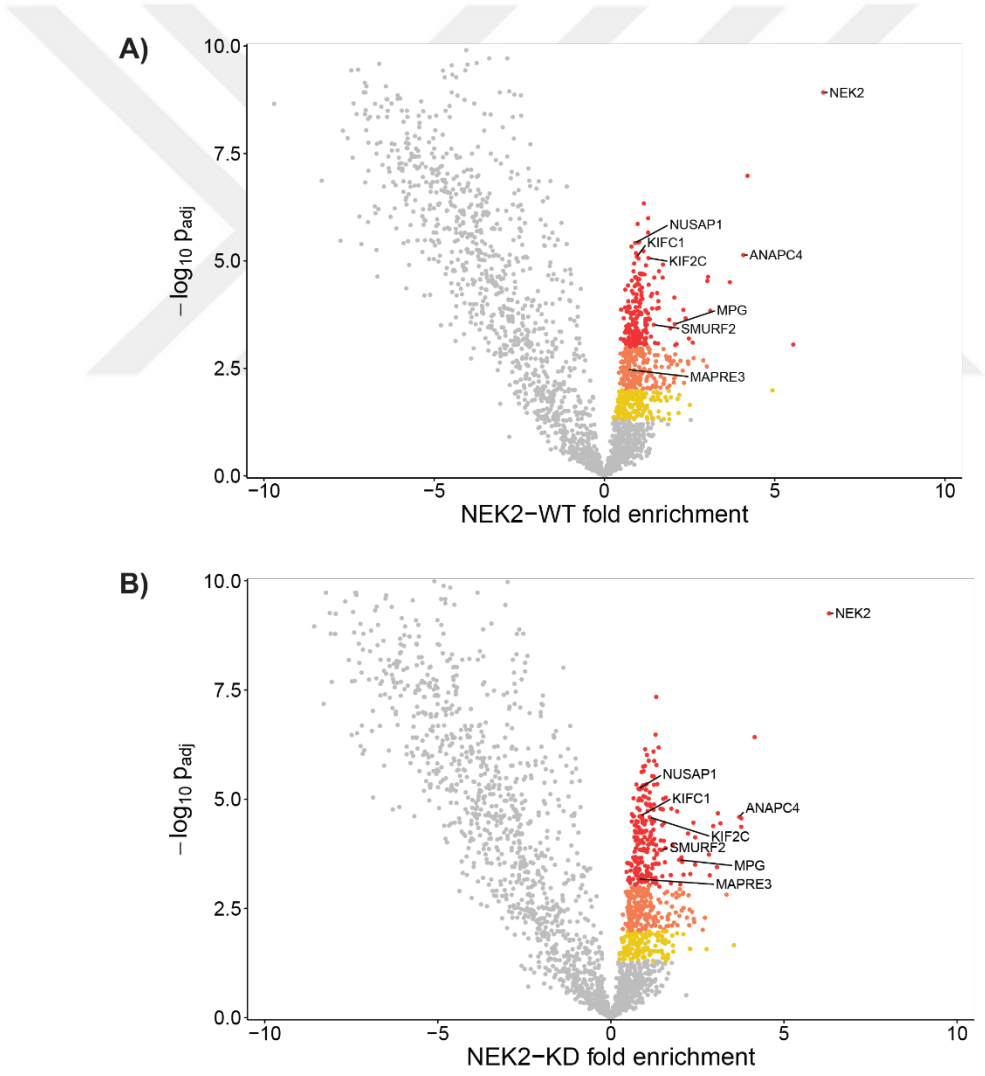

Figure 3-16 Volcano plots of selected proteins in TurboID-Nek2WT (A) and TurboID-Nek2KD (B) samples.

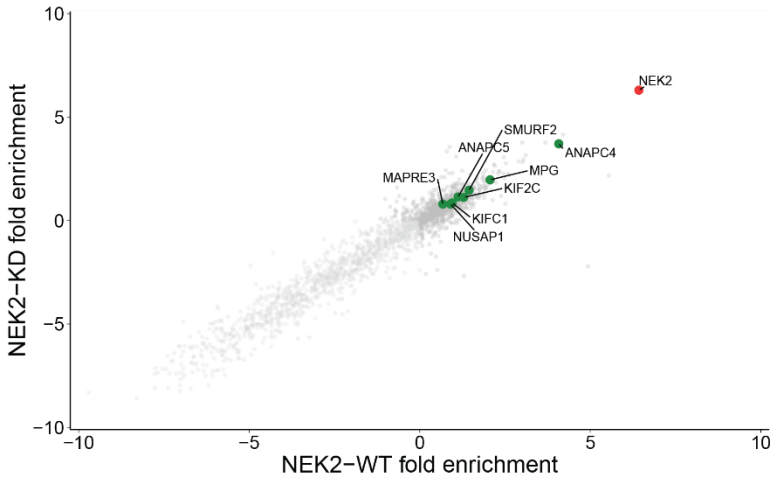

Figure 3-17 Comparative fold change of selected proteins between TurboID-Nek2WT and TurboID-Nek2KD samples.

3.8 Nek2 is a cell cycle regulated protein

Nek2 is a cell cycle regulated protein, hence its expression changes throughout the cell cycle. In line with previous reports, western blot analysis of cells arrested at certain points during the cell cycle showed significant expression changes of Nek2 as expected. To confirm these changes, two synchronization methods were performed; double thymidine block and STLC mitotic arrest.

Treatment with excessive concentration of thymidine arrests cells at G1-S boundary by inhibiting DNA replication. However, to make this arrest sufficient 18 hours of treatment is required for two times. After double thymidine block, cells are arrested at G1-S boundary. By releasing the cells from thymidine cell can continue their cell cycle normally. Therefore, to obtain late S and G2-M cell populations cells were released for 5 h and 10 h respectively.

STLC treatment (10 μM) for overnight was sufficient to arrest cell at M phase. However, mitotic shake was performed after the treatment to get rid of non-arrested cells.

Cyclin E blot, which has the highest concentration at G1-S stages confirmed the synchronization.

After the synchronization anti-Nek2 antibody is used for western blot. Nek2 expression is higher at G1 and G2 stages when compared to S stage. Since Nek2 is degraded via

Anaphase promoting complex during cell division, Nek2 expression was almost non-existent.

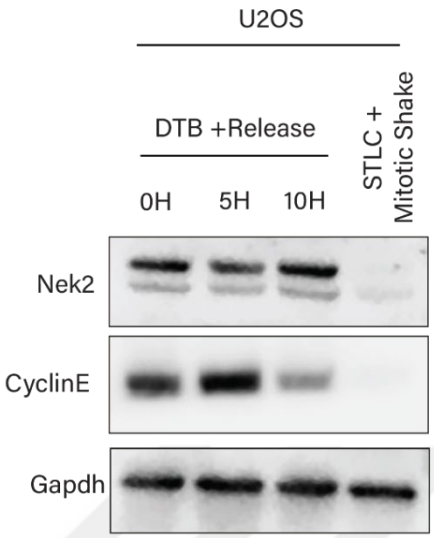

Figure 3-18 Western blot to show Nek2 expression change during cell cycle

Cells are synchronized with double thymidine block (DTB) or STLC. Anti-CyclinE antibody is used to indicate cell cycle stage. Nek2 expression is higher at G2 and G1 compared to S phase and Nek2 is degraded at M phase of the cell cycle.

3.9 Cell cycle synchronisation of TurboID cells

The investigation into Nek2's potential differential interactome at various cell cycle stages was rooted in the understanding that Nek2, as a cell cycle-regulated protein, may undergo dynamic changes in its interactions throughout the cell cycle. To explore this hypothesis, a well-established method involving a double thymidine block was employed to arrest cells at the G1-S boundary.

In this experimental setup, cells were categorized into three groups: the first group was biotinylated at the conclusion of the thymidine block (0H), while the other two groups were biotinylated after release from the thymidine block at 5 and 10 hours, respectively. Notably, the use of the STLC method, which is typically applied for cell synchronization at M phase, was avoided due to Nek2's degradation during the M stage of the cell cycle.

Following the synchronization and biotinylation processes, cells were collected for flow cytometry analysis. Propidium iodide treatment and fixation with 70% ethanol facilitated cell cycle analysis. The results of this analysis revealed the anticipated cell

cycle stage distributions within the various groups: the 0H group predominantly occupied the G1-S boundary, the 5H group was primarily in the late S phase, and the 10H group was predominantly in the G2-M phase. This alignment between the cell cycle stage distributions and the timing of biotinylation validated the effectiveness of the synchronization process.

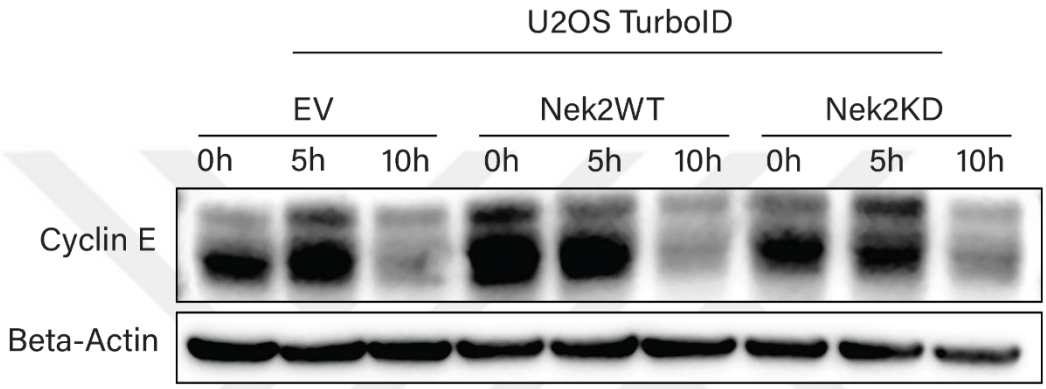

Figure 3-19 Cyclin E blot of cell cycle synchronized TurboID cells.

Cells were synchronized with double thymidine block and released accordingly. Protein samples from each time point were collected and bloted anti-cyclinE antibody. Beta-actin was used for loading control.

To further validate these findings, Cyclin E western blot analysis was conducted on the synchronized cells. As expected, the 0H and 5H groups exhibited notably higher levels of Cyclin E compared to the 10H group, reinforcing the accuracy of intended cell cycle stage at the timing of biotinylation.

The confirmation of TurboID-Nek2 induction in synchronized cells was a critical step in the experimental process. This induction was verified using western blot analysis. The results from this analysis were consistent: all synchronized cells, spanning various cell cycle stages, demonstrated successful expression of TurboID-Nek2 fused constructs.

This crucial validation not only ensured the successful implementation of TurboID-Nek2 but also affirmed that the fusion constructs were effectively expressed within the synchronized cell populations. Such a confirmation is pivotal as it forms the foundation

for subsequent investigations into the dynamic interactions and potential changes in the Nek2 interactome throughout the cell cycle.

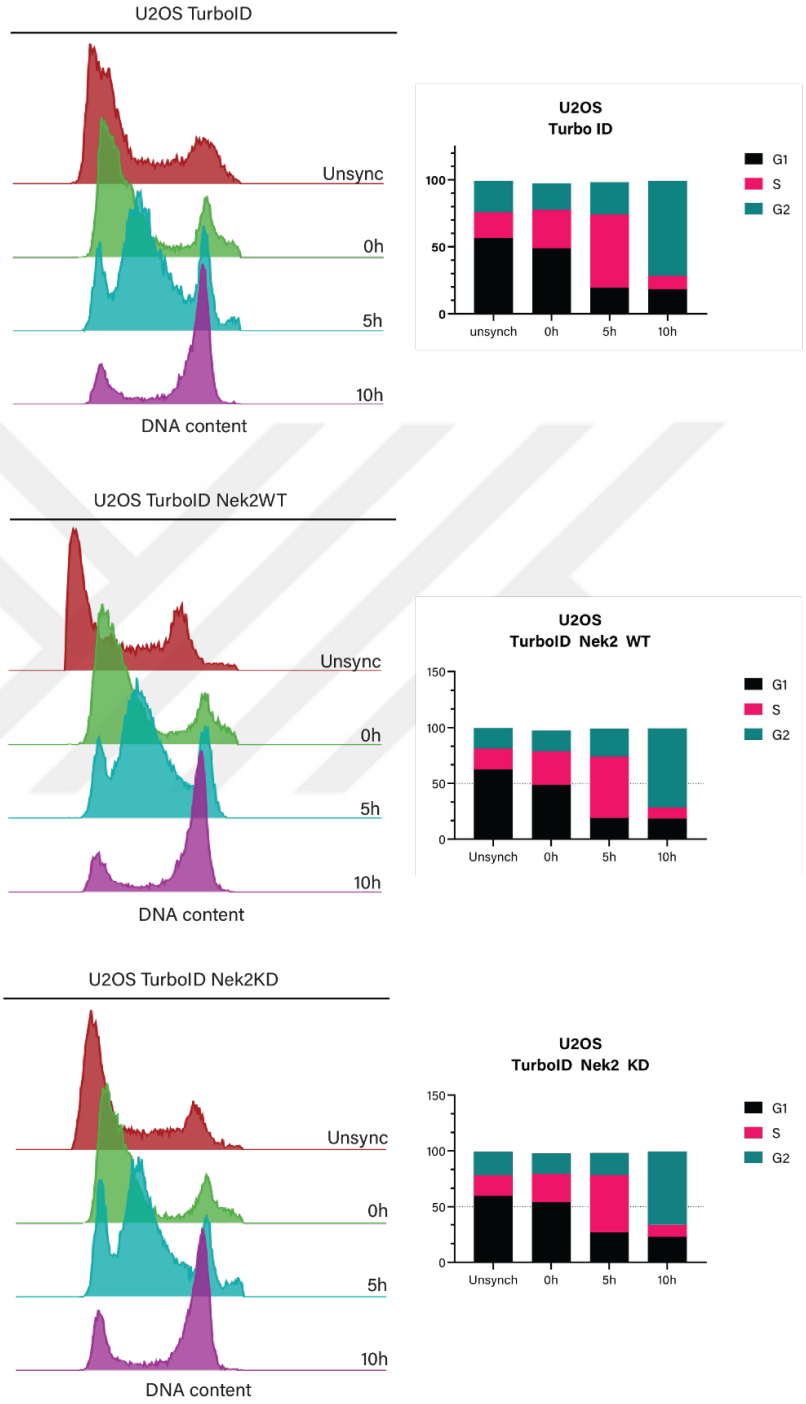

Figure 3-20 Cell cycle analysis TurboID cells with flow cytometry.

TurboID cells are synchronized with double thymidine block at G1/S boundary and released for 0h, 5h, and 10h. Then, cells are fixed at 70% ethanol, and incubated with

Propidium iodide. DNA content is assessed with flow cytometry. Data is visualized with FlowJo software.

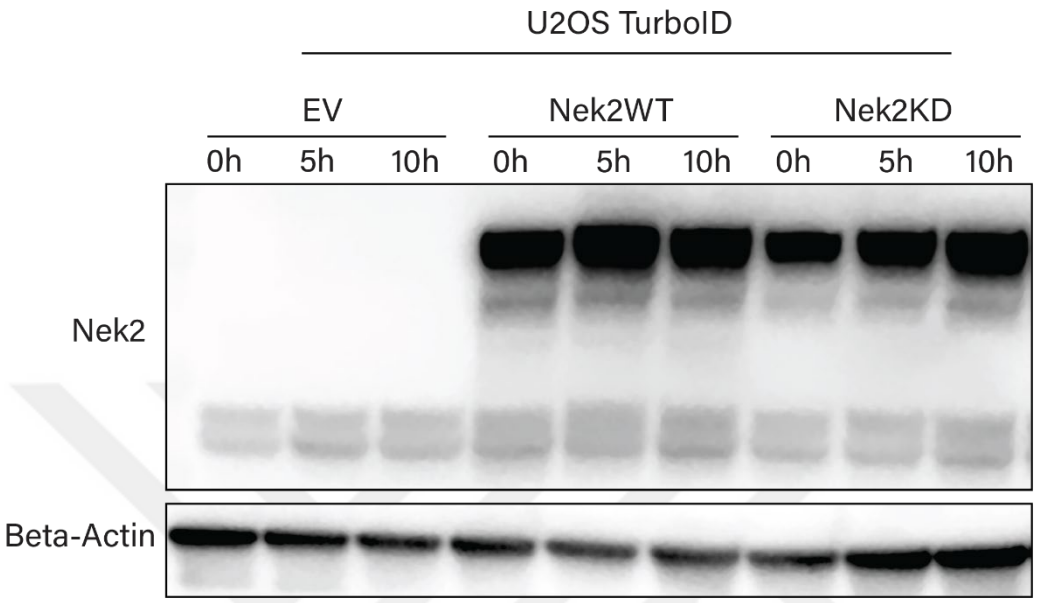

Figure 3-21 *TurboID expression confirmation of synchronized TurboID cells with western blot.*

Synchronized cells are colleted and blotted with anti-Nek2 antibody. TurboID-Nek2WT and TurboID-Nek2KD engineered proteins are expressed after three days of doxycycline induction. Beta-actin is used for loading control.

3.10 Biotinylation confirmation of synchronized cells

The Streptavidin-HRP blotting analysis of synchronized cells yielded results consistent with those observed in unsynchronized cells, highlighting key findings in the study. Notably, EV-TurboID cells exhibited significantly higher levels of biotinylation when compared to TurboID-Nek2WT and TurboID-Nek2KD cells. However, it's worth emphasizing that all cell groups, regardless of their TurboID construct, displayed successful biotinylation of proteins within a 30-minute interval.

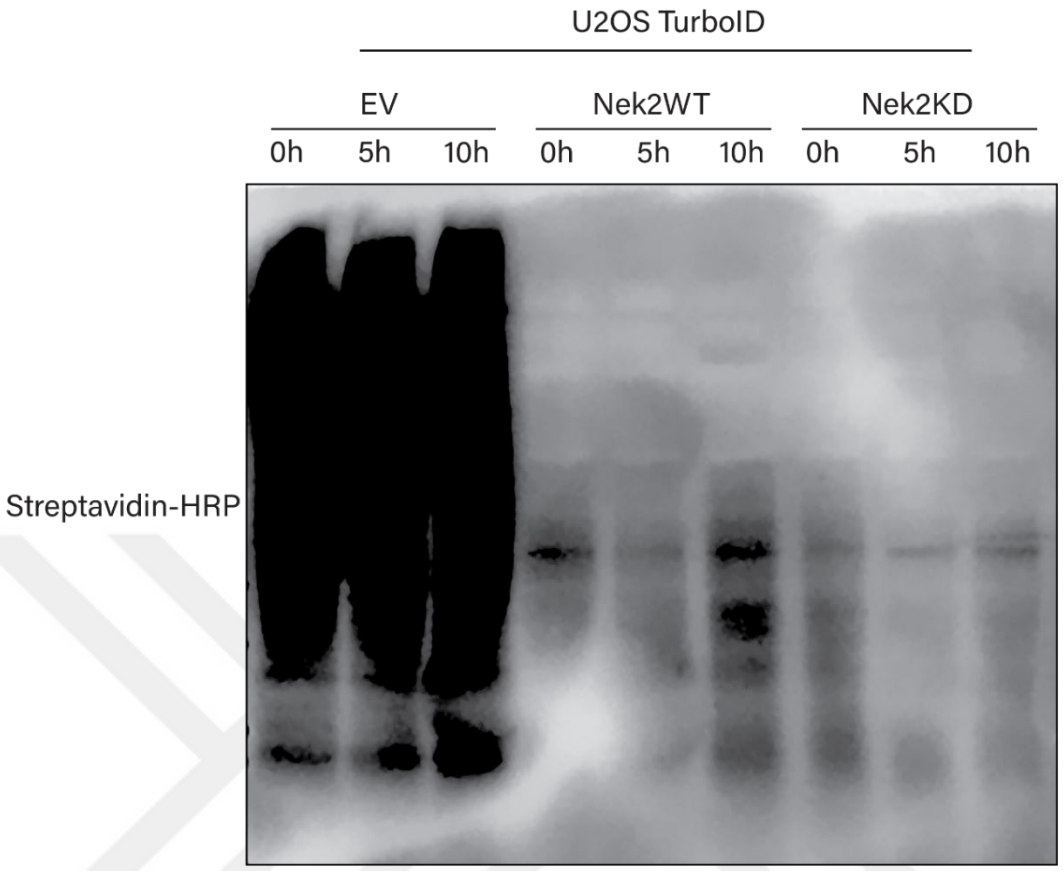

Figure 3-22 Streptavidin-HRP blot of synchronized biotinylated TurboID cells

Cell cycle synchronized TurboID cells were biotinylated right before pellet collection for 30 minutes with 500uM d-biotin. Proteins isolated from cell pellets were blotted with streptaividin-HRP. TurboID control shows excessive amounts of biotinylation when compared to TurboID-Nek2 groups.

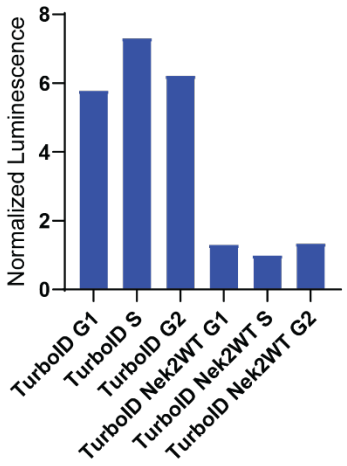

Figure 3-23 Quantitative analysis of total biotinylation of TurboID cells with direct-ELISA (Sterptavidin-HRP)

Total biotinylation of EV-TurboID and TurboID-Nek2WT cells were analysed with direct enzyme-linked immunosorbent assay (direct-ELISA).

These findings underscore the consistent patterns of biotinylation observed across synchronized and unsynchronized cell populations. The elevated biotinylated protein levels in EV-TurboID cells, in contrast to TurboID-Nek2WT and TurboID-Nek2KD cells, reaffirm the functional differences in biotin ligase activity. Additionally, the centrosome-centric biotinylation of proteins suggests the intriguing possibility of Nek2's involvement in this vital cellular structure throughout the cell cycle, further emphasizing its potential regulatory roles in diverse cellular processes.

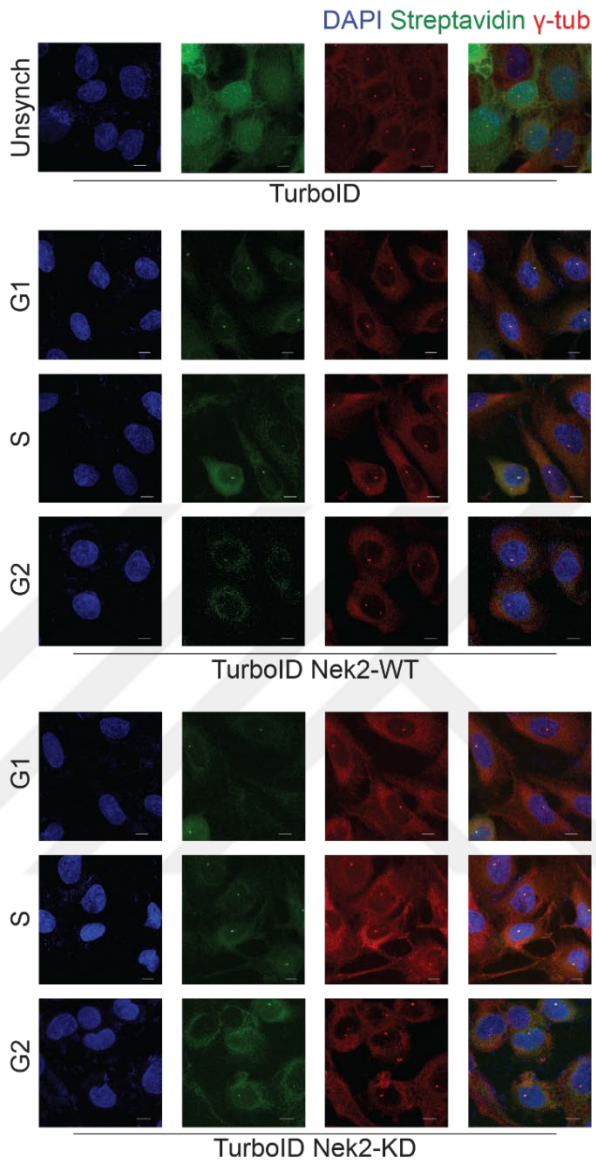

Figure 3-24 Immunofluorescence imaging of biotinylation at different cell cycle steps with streptavidin-488 and anti-gamma tubulin.

TurboID-Nek2WT and TurboID-Nek2KD cells are biotinylated and biotinylation is imaged with streptavidin-488. Biotinylated proteins are mostly accumulated at centrosomes for each cell cycle steps. Confocal microscopy (Leica DMI8/SP8 Confocal System) was used.

3.11 Mass Spectrometry analysis of synchronized TurboID mediated proximity labelling

Following the confirmation of the successful translation of TurboID constructs and their subsequent biotinylation at expected target regions at different cell cycle steps, a substantial number of cells were synchronized with double thymidine block and biotinylated for 30 minutes right before pellet collection. Their protein content was isolated and biotinylated proteins were isolated through an affinity purification process employing streptavidin-coated resin beads. The enriched proteins obtained from this pulldown were subjected to analysis via liquid chromatography-mass spectrometry (LC-MS).

The raw data originating from the Thermo MS instrumentation were subjected to analysis using the MaxQuant software just as unsynchronized samples. MaxQuant facilitated the comparative examination of different experimental groups, enabling the normalization of protein intensities across the groups. Following the MaxQuant analysis of the mass spectrometry data, notable disparities between the Nek2 groups and the TurboID-EV group became evident for all cell cycles. These disparities manifested in terms of both protein quantities and their corresponding intensities, which exhibited substantial discrepancies. The extent of this dissimilarity posed a hindrance to the straightforward application of statistical analyses since there are 9 different experimental groups.

To mitigate the challenges posed by the substantial inter-group differences, an imputation methodology was employed. The Cassiopeia program was utilized for this purpose, resulting in the implementation of imputation strategies that rendered all experimental groups comparable without exerting undue influence on the subsequent analyses. Subsequent to the imputation process, statistical analysis was conducted using the limma framework.

Intensity heatmap for all cell cycle and TurboID groups reveals difference of TurboID-Nek2KD-G2 compared to other groups.

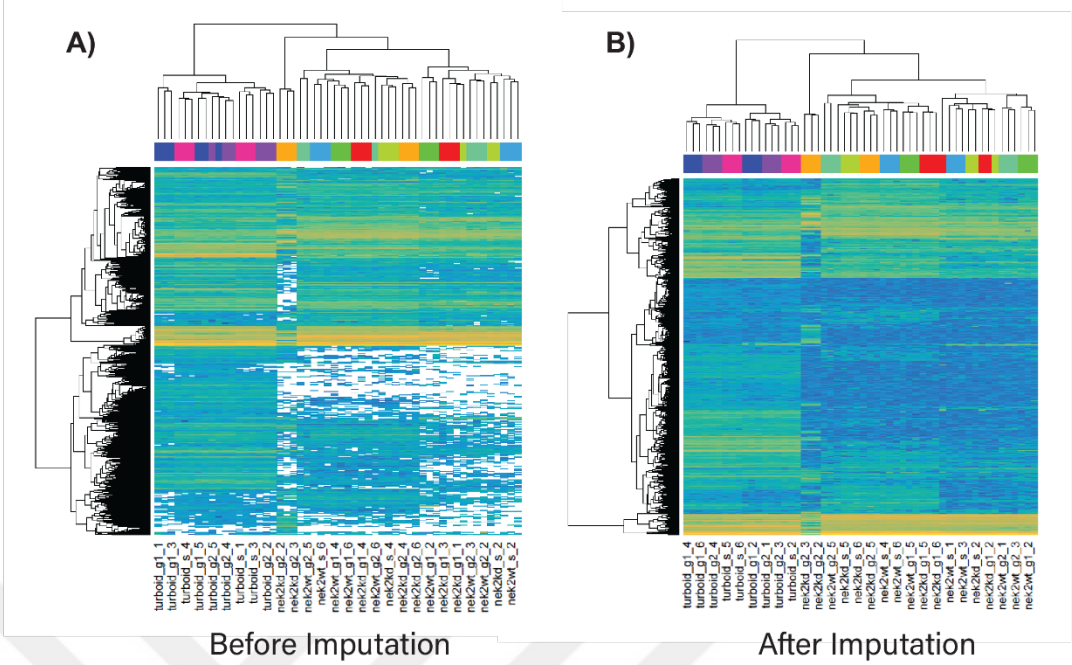

Figure 3-25 Normalized intensities of detected proteins at synchronized samples before and after imputation.

(A) Before the imputation substantial amount of proteins detected at TurboID control group were missing at Nek2WT and NekwKD groups.

(B) Imputation normalized the distribution of total proteins for a relevant statistical analysis.

After the statistical analysis all cell cycle steps were compared to each other with a Venn diagram for both Nek2WT and Nek2KD groups. 165 proteins were commonly enriched at G1, S, and G2 groups for Nek2WT. On the other hand, 109 proteins were commonly enriched at G1, S, and G2 groups for Nek2KD. For Nek2WT, 110 proteins were only enriched at G1 stage, 26 proteins were only enriched at S stage, and 24 proteins were only enriched at G2 stage. For Nek2KD, 52 proteins were only enriched at G1 stage, 37 proteins were only enriched at S stage, and 141 proteins were only enriched at G2 stage. Excessive amounts of Nek2KD G2 specific proteins is consistent with imputation heatmap.

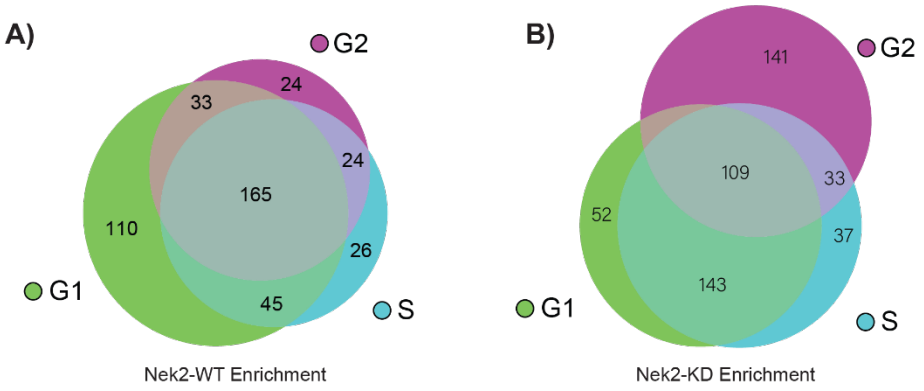

Figure 3-26 Venn diagram for G1, S, and G2 phases for TurboID-Nek2WT (A) and TurboID-Nek2KD samples (B).

Significantly enriched proteins for each cell cycle were compared. 165 and 109 proteins were enriched at all cell cycle steps for Nek2WT and Nek2KD respectively.

Unsynchronized and synchronized mass spectrometry analyses were conducted to compare the composition of Nek2WT and Nek2KD. Remarkably, the results indicated a high degree of similarity between these two variants concerning their composition. This suggests that the kinase activity of Nek2 does not significantly impact its positional dynamics and interactions with other proteins.

A fold change comparison of target proteins, as derived from unsynchronized mass spectrometry data across distinct cell cycle stages, was graphically represented using a heatmap. The overall distribution of these proteins exhibited negligible differences among the various cell cycle stages, with the exception of Mapre3 and Kif2c. These proteins consistently maintained close proximity to Nek2 throughout all observed cell cycle stages, indicating their consistent interaction.

To gain further insights, a pathway analysis was performed specifically for Nek2WT during G1, S, and G2 phases, employing the shinyGO tool. Notably, the enriched pathways encompassed Ribosome, Coronavirus disease, Cell cycle, and Ubiquitin Mediated Proteolysis. Remarkably, these pathways remained consistently enriched across all cell cycle stages, suggesting that Nek2's immediate microenvironment exhibits remarkable stability throughout the cell cycle.

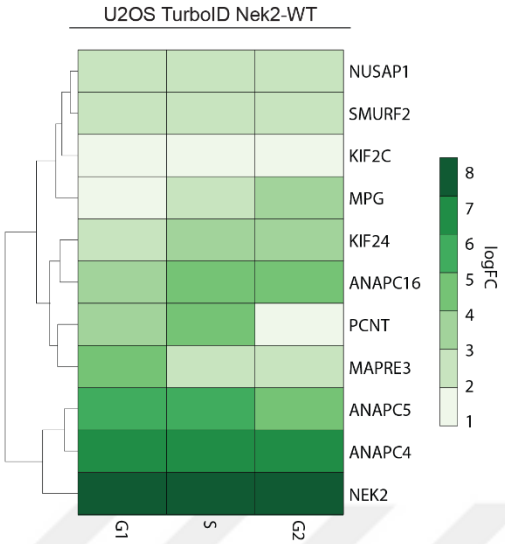

Figure 3-27 Heatmap of TurboID-Nek2WT enrichment fold change for G1, S, and G2 cell cycle steps.

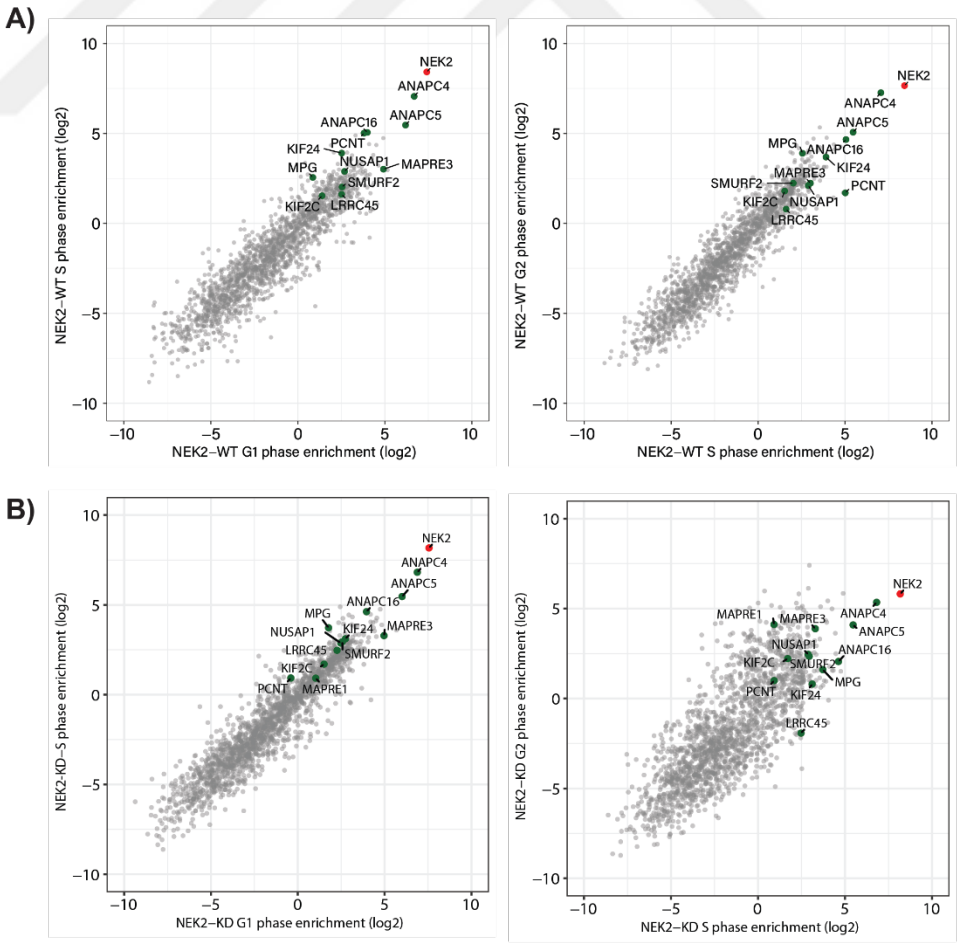

Figure 3-28 Comparative fold change of selected proteins between G1-S and S-G2 for TurboID-Nek2WT (A) and TurboID-Nek2KD (B) samples.

There is no significant difference for Nek2WT and Nek2KD samples.

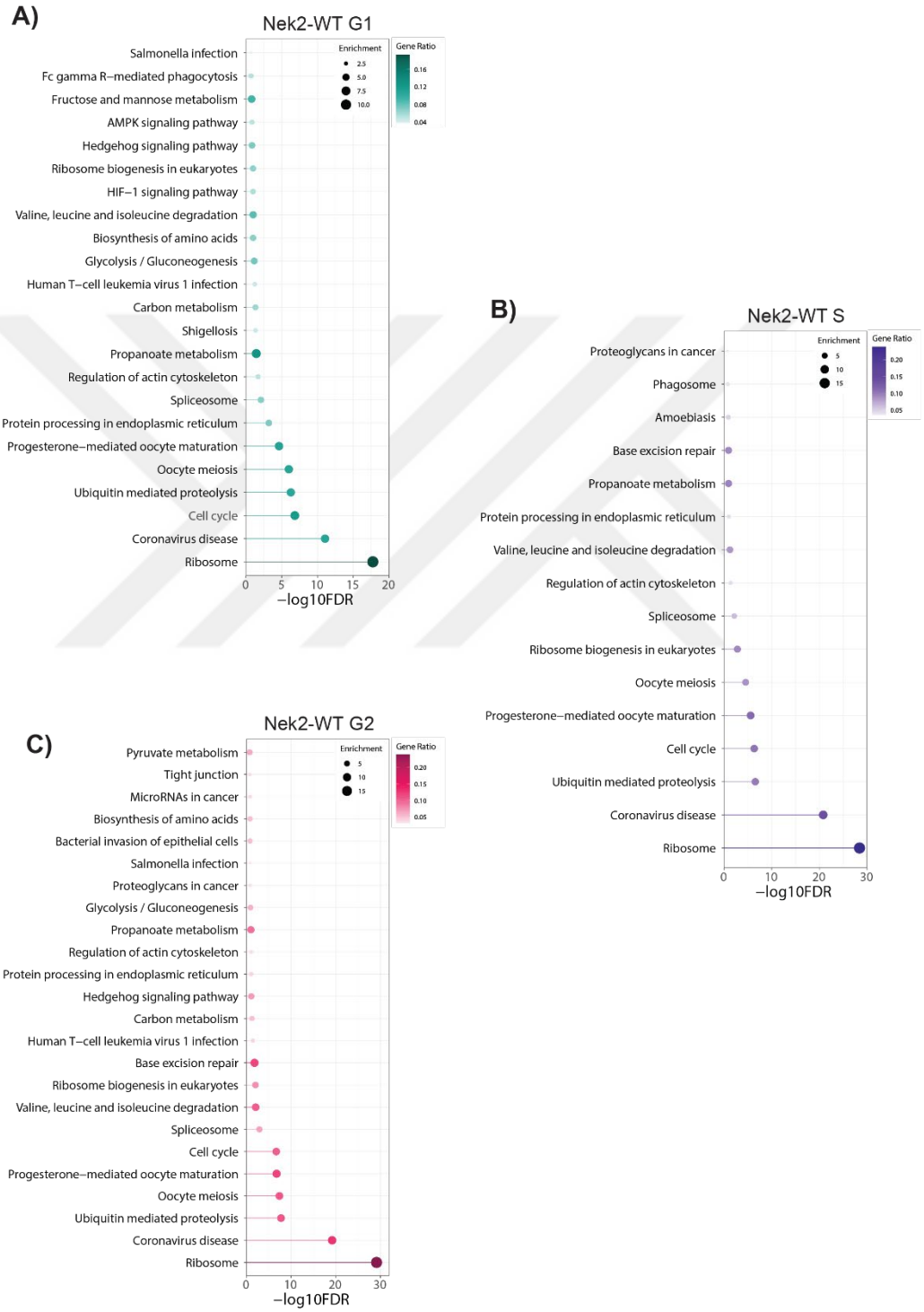

Figure 3-29 KEGG-Pathway analysis of significantly enriched proteins at Nek2WT cell cycle steps G1 phase (A), S phase(B), and G2 phase (C)

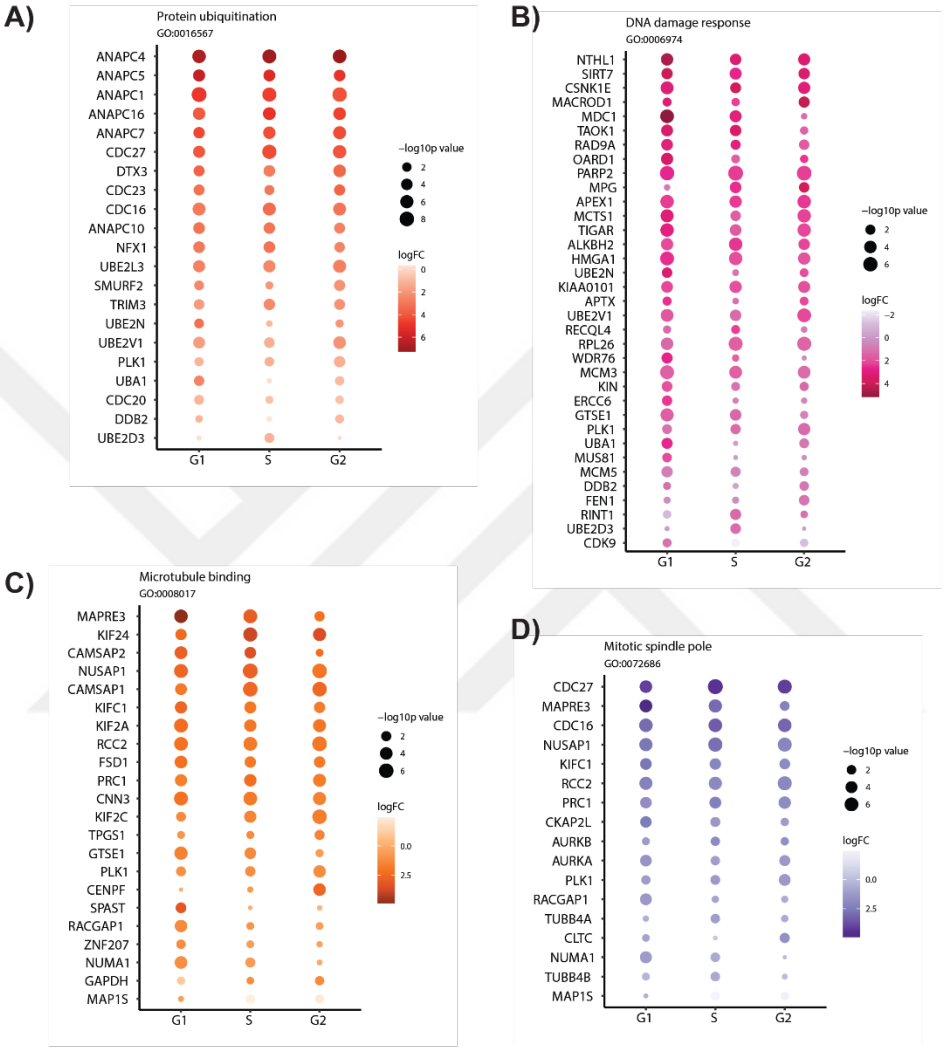

Figure 3-30 Individual proteins that are significantly enriched in Nek2WT group that are a part of following GO-Terms; Protein Ubiquitination (A), DNA Damage Response (B), microtubule binding (C) and Mitotic Spindle pole (D) for G1, S, and G2 phases.

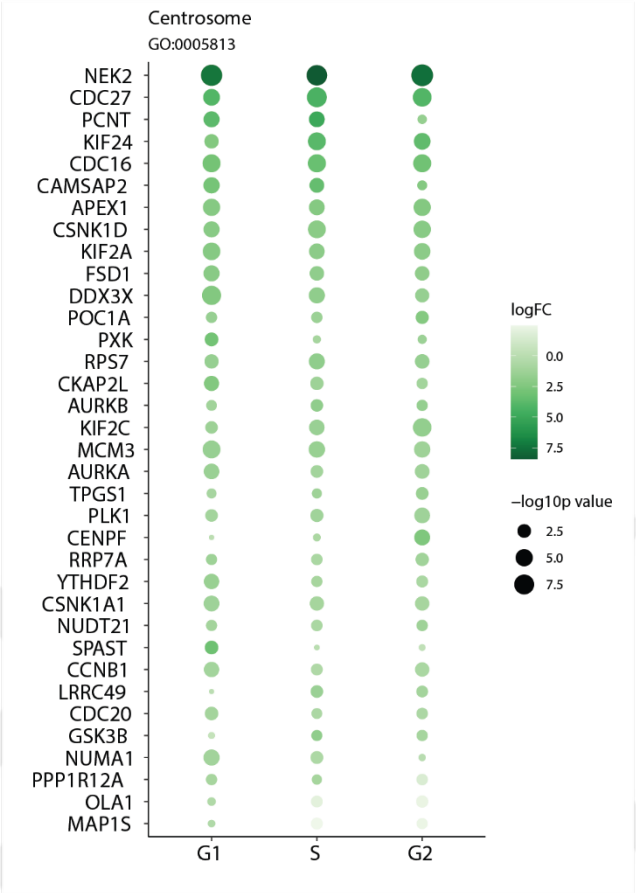

Figure 3-31 Individual proteins that are significantly enriched in Nek2WT group that are a part of Centrosome GO-term for G1, S, and G2 phases.

Further examination of the proteins that exhibited significant enrichment within various Gene Ontology (GO) terms unveiled a substantial presence of proteins associated with distinct cellular functions. Notably, these functions encompassed Centrosome, Protein Ubiquitination, DNA Damage Response, microtubule binding, and Mitotic Spindle pole.

For the GO term related to the cilium, noteworthy proteins included Camsap2, Cfap20, Csnk1d, and Kif2a. Their presence in this context suggested potential involvement in cilium-related functions, which encompass critical roles in cellular sensory perception and signaling.

In the context of the Ubiquitin GO term, prominent candidates were Anaphase promoting complex (APC) and Smurf2. The inclusion of these proteins underscores their potential roles in mediating protein degradation, post-translational modifications, and cellular signaling cascades through ubiquitin pathways.

For the Mitotic Spindle GO term, Cdc27, Mapre3, Cdc16, and Nusap1 emerged as significant participants. Their association with this GO term suggests their involvement in orchestrating mitotic spindle dynamics, an essential aspect of cell division.

Similarly, for the Microtubule Binding GO term, the presence of proteins such as Mapre3, Kif24, Camsap2, and Nusap1 indicates their roles in regulating microtubule dynamics and organization, pivotal for various cellular processes including intracellular transport and structural integrity.

In the context of the Centrosome GO term, proteins like Cdc27, Pcnt, Kif24, and Cdc16 gained prominence, hinting at their potential contributions to centrosome-associated functions, crucial for cellular organization and division.

Lastly, within the DNA Damage Response GO term, notable participants included Nthl1, Sirt7, Csnk1e, and Mpg. Their presence underscores their potential roles in maintaining genome stability, orchestrating DNA repair pathways, and regulating cellular responses to DNA damage.

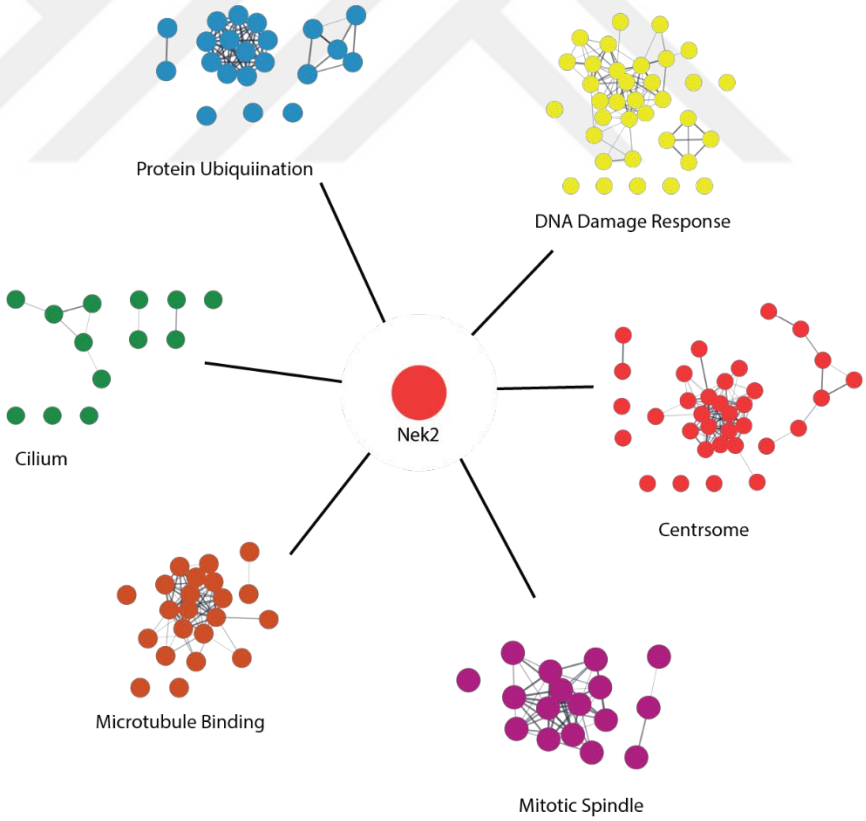

Figure 3-32 String analysis of significantly enriched proteins at selected GO-Term analysis.

Western blot confirmation of Mass Spec results

Selected proteins identified through mass spectrometry were subjected to validation through western blot analysis for both synchronized and unsynchronized cell samples. Following the biotinylation of the samples, cellular material was collected, and protein content was extracted. Unlike the mass spectrometry approach where beads were digested, a different protocol was employed for pulldown samples. In this protocol, 4x Laemmli buffer with DTT was utilized to facilitate the separation and denaturation of the pulldown samples. These denatured samples were subsequently used directly for western blot analysis.

Initially, the focus was on evaluating the enrichment of proteins across all cell phases, including unsynchronized data. Regrettably, the results from the total pulldown experiments did not successfully demonstrate the enrichment of the target proteins. Interestingly, EV-TurboID, which typically exhibits more pronounced total biotinylation, demonstrated comparable or greater pulldown efficiency of target proteins compared to TurboID-KD and TurboID-WT samples.

Given the challenge of directly comparing total biotinylated proteins due to the substantial disparity in EV-TurboID's total biotinylation, an alternative strategy was devised. This approach aimed to mimic the normalization steps commonly applied in mass spectrometry analysis. Instead of assessing total pulldown across different samples, the fraction of biotinylated target protein relative to the total biotinylation within each group was assessed. To achieve this, loaded samples were normalized based on their total biotinylated protein content from Streptavidin-HRP ELISA.

The evaluation of protein enrichment through biotinylation revealed that the fraction of biotinylated Nusap1, Kif2c, Mpg, Kif2a, Mapre3, and Smurf2 in TurboID-Nek2WT and TurboID-Nek2KD samples surpassed that observed in EV-TurboID samples. In contrast, Rab6, Dek, Cenpf, and Taok1 exhibited no noticeable enrichment in unsynchronized samples.

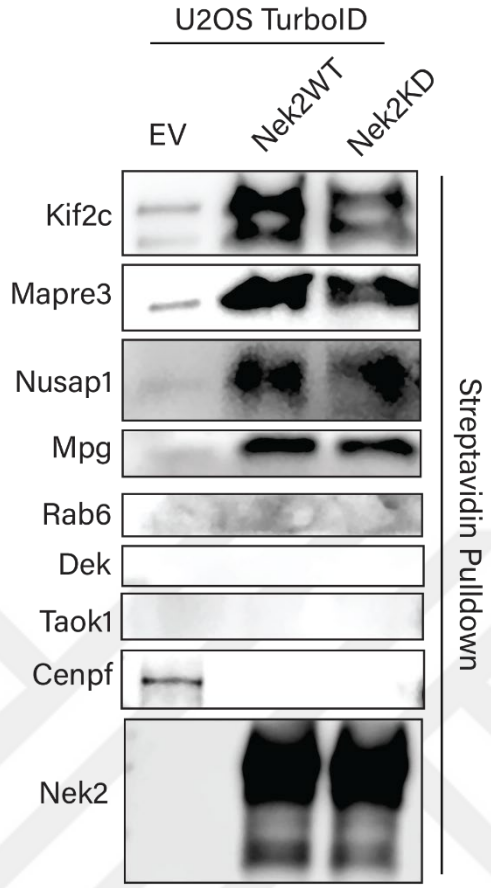

Figure 3-33 Western blot confirmation of unsynchronized biotinylation of selected proteins after Streptavidin pulldown.

Samples are normalized with ELISA and pulled down with streptavidin resin beads and blotted with selected antibodies.

Applying a similar approach to synchronized samples, the overall biotinylation levels for synchronized samples were quantified using ELISA as well. Subsequently, normalization to total biotinylation was carried out for G1, S, and G2 samples from both EV-TurboID and TurboID-Nek2WT groups. Western blot analysis was then conducted. Notably, in TurboID-Nek2WT samples, Nusap1, Kif2c, Kif2a, and Mpg demonstrated enrichment compared to EV-TurboID samples. The fractions of biotinylated proteins in TurboID-Nek2WT and TurboID-Nek2KD samples surpass those in the EV-TurboID sample, indicative of their significant interaction with Nek2.

In summary, this comprehensive analysis further substantiates the intricate interplay between Nek2 and its interacting proteins. The differential enrichment patterns

in both unsynchronized and synchronized contexts shed light on the dynamic nature of these interactions and provide valuable insights into their cell cycle-dependent dynamics.

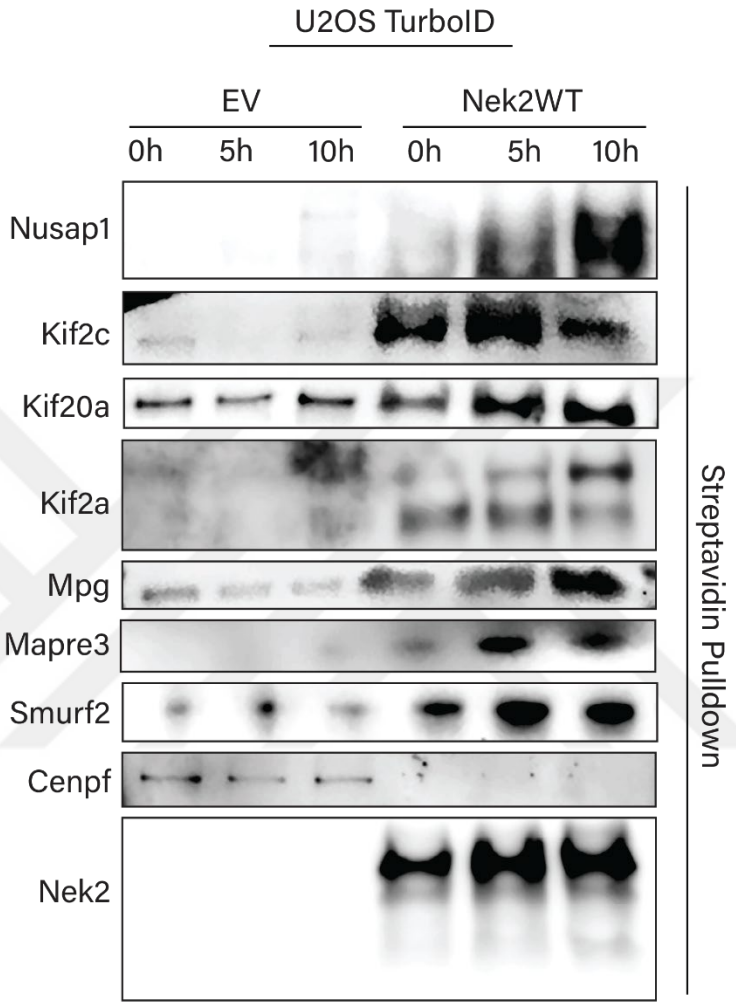

Figure 3-34 Western blot confirmation of synchronized biotinylation of selected proteins after Streptavidin pulldown.

Synchronized samples were normalized with ELISA and pulled down with streptavidin resin beads and blotted for indicated antibodies.

3.12 Coimmunoprecipitation by FLAG-Nek2 pulldown

Upon successful validation of the mass spectrometry findings through western blot analysis in both unsynchronized and synchronized samples, a more detailed exploration of the interactions involving the target proteins was undertaken utilizing coimmunoprecipitation.

For this purpose, U2OS cells engineered with HA-FLAG-Nek2, as developed by Batuhan Mert Kalkan, were employed to facilitate the pulldown of Nek2. In order to maintain the structural integrity of the protein complexes, IP lysis buffer was utilized during the pulldown process. Given that coimmunoprecipitation involves multiple non-covalent interactions, paraformaldehyde (PFA) fixation was employed to stabilize the protein clusters, thereby preserving their spatial relationships.

Following the FLAG pulldown, the target proteins that exhibited close proximity to Nek2 were identified and subsequently subjected to blotting using specific antibodies. Remarkably, Kif2c, Mapre3, Mpg, Nusap1, and Smurf2 displayed enrichment in the Nek2 pulldown samples. This enrichment strongly indicates a direct binding between these proteins and Nek2, elucidating their interaction within cellular context.

Furthermore, the validation of Nusap1 interaction was established independently, without the necessity of utilizing PFA fixation. This additional verification underscores the robustness of the observed interactions and reinforces the credibility of the coimmunoprecipitation methodology.

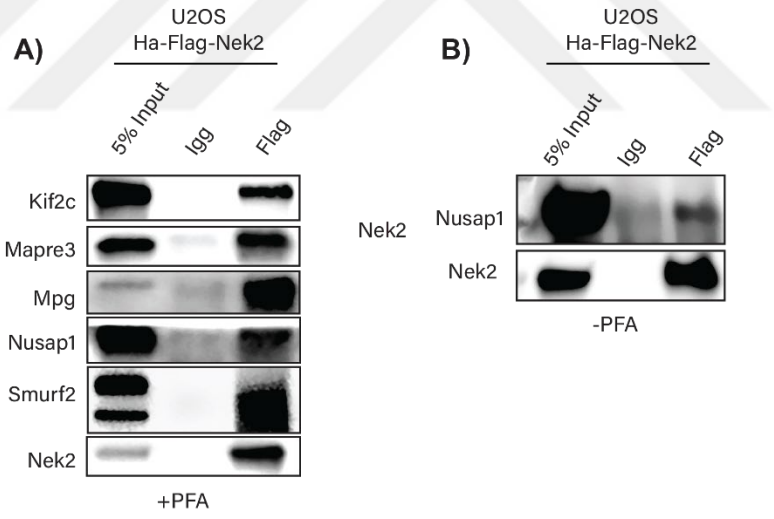

Figure 3-35 Coimmunoprecipitation by FLAG-Nek2 pulldown, with PFA fixation (A), and without PFA fixation (B)

Kif2c, Mapre3, Mpg, Nusap1, and Smurf2 directly binds to Nek2.

With Batuhan Mert Kalkan

3.13 Colocalization with Nek2

To comprehensively investigate the interactions of the target proteins, immunofluorescence imaging was employed as a valuable tool. Given Nek2's predominant localization at the centrosome, the initial step involved verifying the centrosomal localization of the target proteins. This was achieved using endogenous antibodies coupled with anti-gamma tubulin staining. Intriguingly, Ckap4, Mapre3, Smurf2, Nsun4, Kif20a, and Mark3 demonstrated colocalization with gamma tubulin, conclusively confirming their centrosomal localization.

Subsequent to confirming centrosomal localization, the focus shifted to evaluating their colocalization with Nek2. To achieve this, U2OS cells engineered with HA-FLAG-Nek2 were employed. HA-tagging facilitated the visualization of Nek2, while the use of endogenous antibodies enabled the visualization of the target proteins.

Interestingly, Mpg and Nusap1 exhibited colocalization with Nek2 at the nucleus, suggesting a potential association within this cellular compartment. On the other hand, Ckap4, Mapre3, Nsun4, Kifc1, and Mark3 demonstrated colocalization with Nek2 at centrosomes or spindle structures. This striking pattern of colocalization underscores the intricate nature of the interactions between these target proteins and Nek2, implicating their involvement in diverse subcellular processes.

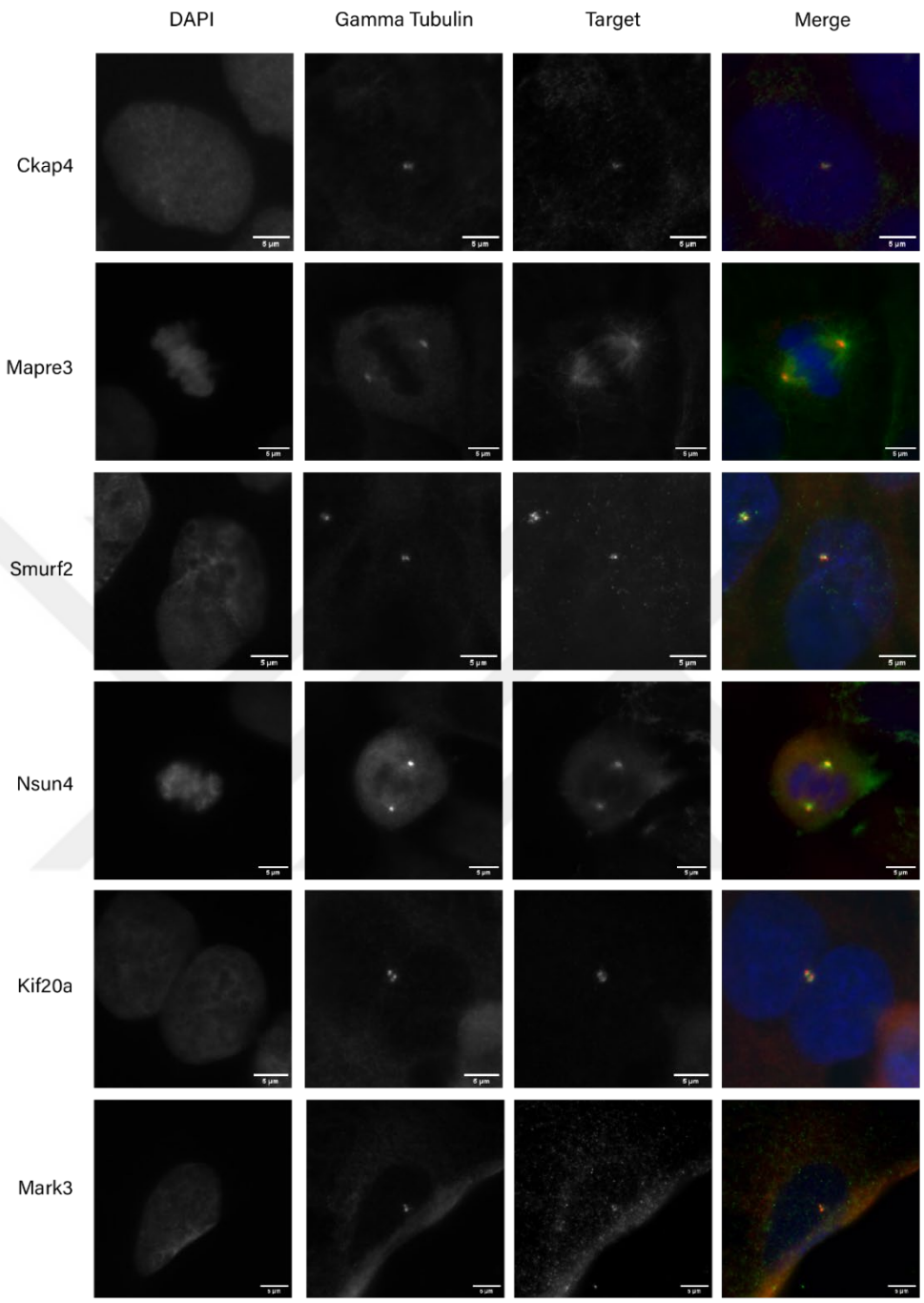

Figure 3-36 Some target proteins are localized at centrosomes

Ckap4, Mapre3, Smurf2, Nsun4, Kif20a, and Mark3 colocalized with gamma tubulin, indicating centrosomal localization. Immunofluorescence imaging performed with endogenous antibodies. Methanol fixation was used.

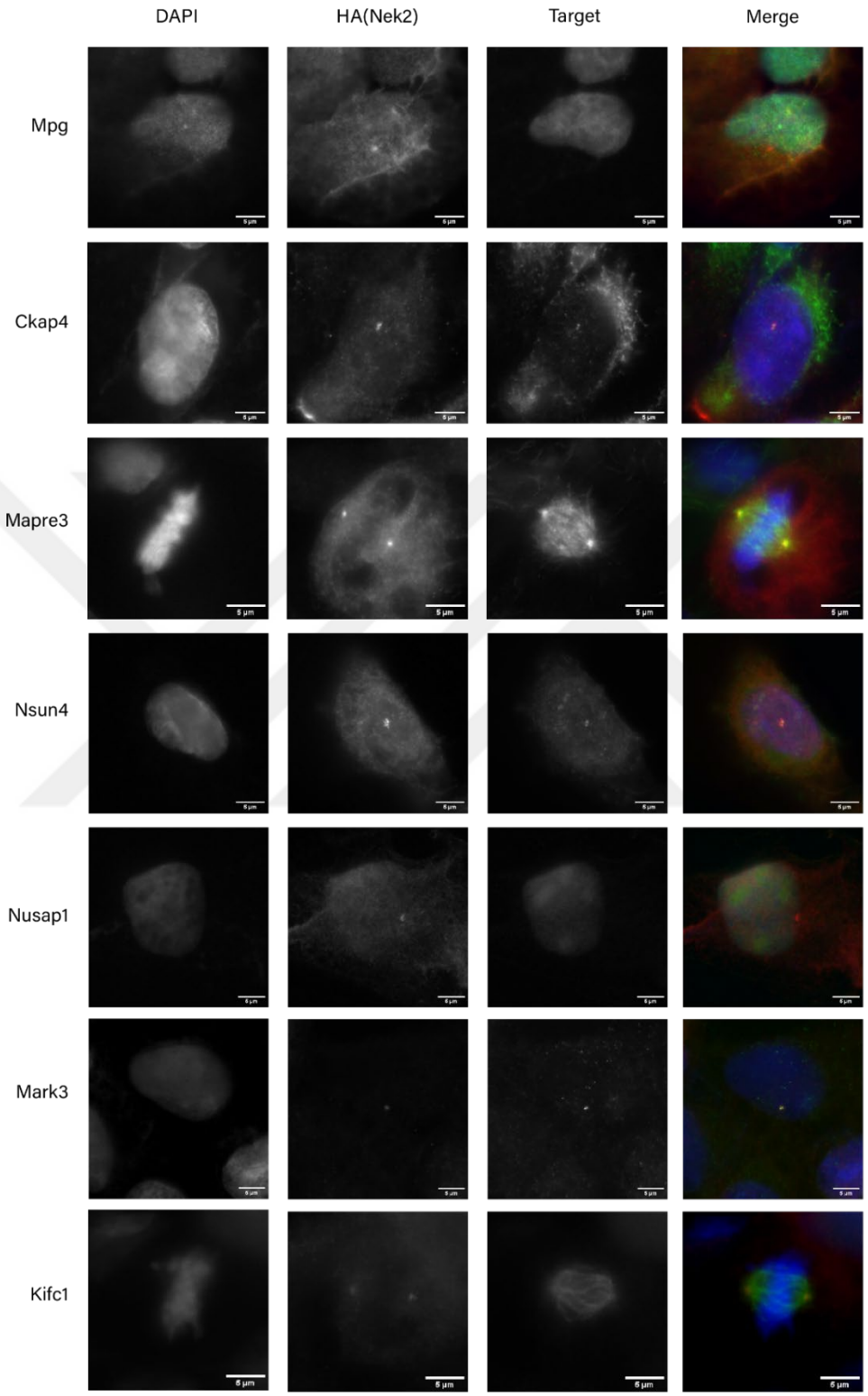

Figure 3-37 Colocalization of Nek2 and target proteins.

Mpg and Nusap1 colocalized with Nek2 at the nucleus, while Ckap4, Mapre3, Nsun4, Kifc1 and Mark3 colocalized with Nek2 at the centrosomes or spindle.

Methanol fixation was used for Ckap4, Mapre3, Nsun4, Kifc1 and Mark3 IF.

PFA fixation was used for Mpg and Nusap1 IF.

3.14 Generation of Nek2KO cell lines

To investigate the functional implications of Nek2 in conjunction with the target proteins, a crucial step involved the generation of Nek2 knockout (KO) cell lines. This was accomplished through the application of the Crispr-Cas9 gene editing technology. U2OS cells were subjected to viral transduction with a lentiviral vector containing Nek2-specific guide RNA sequences, embedded within the lentiCRISPR v2 plasmid. Subsequent to transduction, the cells underwent a selection process using puromycin to isolate a pool of cells. The aim was to obtain a population in which Nek2 had been effectively disrupted.

However, upon assessing the Nek2 content of the selected cells through western blot analysis, no substantial decrease in Nek2 expression was observed following viral transduction. The cells were seeded into a 96-well plate, facilitating the cultivation of single colonies. Approximately 40 colonies were screened to ascertain their Nek2 expression levels.

In this rigorous screening process, two distinct colonies, designated as B5 and B9, were identified as Nek2 knockout cell lines. These cell lines served as the foundation for subsequent investigations aimed at elucidating the functional roles of Nek2 in association with the target proteins.

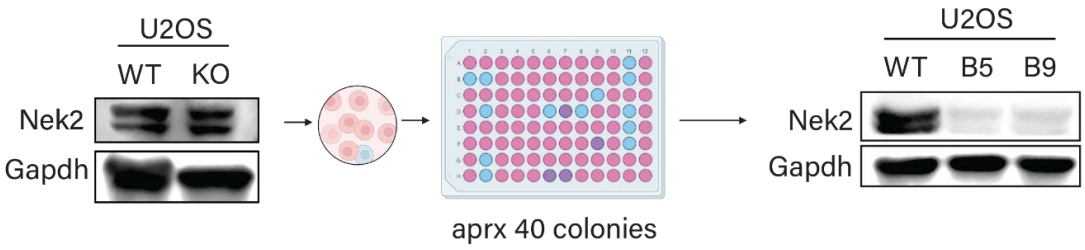

Figure 3-38 Generation scheme of U2OS Nek2 KO cell lines.

Nek2 was knocked out via viral transduction. Approximately 40 single colonies were screened with western blot. Two colonies, B5 and B9 were confirmed as Nek2 KO cell lines.

Table 2 Nek2 KO guides

NEK2-guide2-F	caccGACATCGTTCGTTACTATGAT
NEK2-guide2-R	aaacATCATAGTAACGAACGATGTC

3.15 Nusap1 is upregulated when Nek2 is depleted.

The protein expression profile of Nusap1, a protein previously identified as directly binding to Nek2, exhibited a significant upregulation in Nek2 knockout (Nek2KO) cell lines. This observation was consistently replicated when Nek2 was depleted using siRNA treatment. Given that the reduction of Nek2 was consistently associated with increased Nusap1 protein levels, a reciprocal relationship was hypothesized. However, considering that Nusap1 is an essential gene, complete degradation upon Nek2 overexpression was deemed unlikely. As expected, when Nek2 was overexpressed, Nusap1 levels displayed a modest increase.

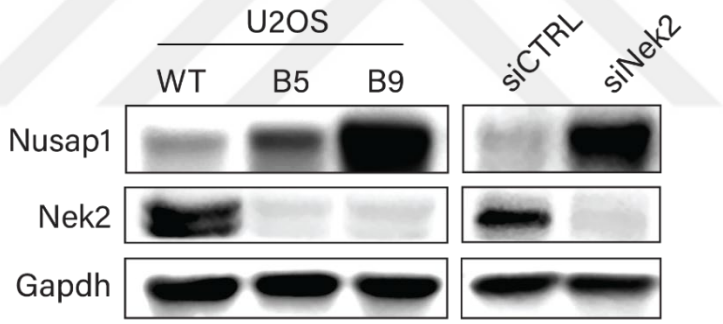

Figure 3-39 Nusap1 is upregulated at Nek2KO and siNek2 treated cell lines.

Intrigued by the hypothesis that Nek2 might function as a negative regulatory factor for Nusap1 expression, a systematic approach was undertaken. Nek2 overexpression was triggered in a temporally controlled manner, and Nusap1 expression was monitored throughout this period. Remarkably, the initiation of Nek2 overexpression resulted in an initial depletion of Nusap1 expression, aligning with the hypothesis. However, a noteworthy phenomenon emerged, revealing that Nusap1 levels rebounded between 4 to 6 hours of continuous Nek2 overexpression.

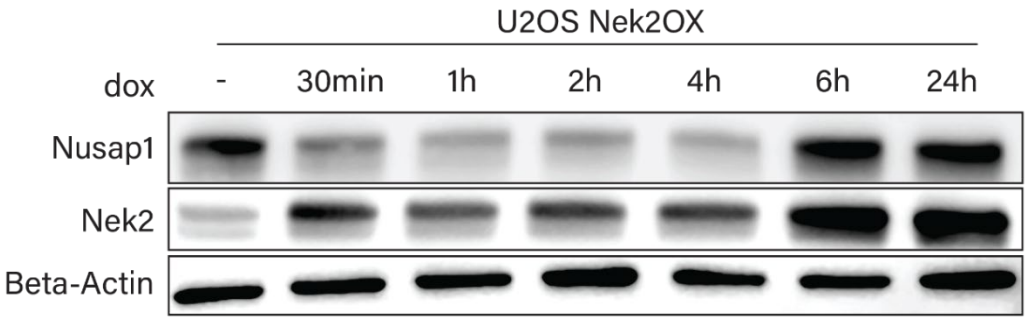

Figure 3-40 Nusap1 is downregulated at first 6 hours of Nek2 overexpression.

This intriguing observation signifies the complexity of the regulatory interplay between Nek2 and Nusap1. The initial depletion followed by a subsequent recovery of Nusap1 expression upon Nek2 overexpression suggests a nuanced and dynamic relationship between these two proteins. This temporal effect highlights the intricate mechanisms governing their interaction and the regulatory processes influencing Nusap1 expression.

3.16 Nek2 causes degradation of Nusap1 by inducing ubiquitin mediated proteolysis.

The expression of Nek2 was found to exert a negative regulatory influence on Nusap1 protein levels. This observation led to the hypothesis that Nek2's regulatory mechanism involves phosphorylation-mediated ubiquitination of Nusap1. To delve deeper into this hypothesis, a cycloheximide chase assay was strategically employed.

The cycloheximide chase assay operates on the principle of inhibiting protein translation by blocking ribosomal synthesis. This inhibition of protein synthesis allows the remaining protein concentration to serve as an indicator of stability against proteasomal degradation. Employing this approach, it was revealed that Nusap1 displayed greater resistance to proteasomal degradation in U2OS Nek2 knockout (KO) cells compared to U2OS wild-type (WT) cells. This result strongly supports the

hypothesis that Nek2 serves as a regulatory element for Nusap1 through the proteasomal degradation pathway.

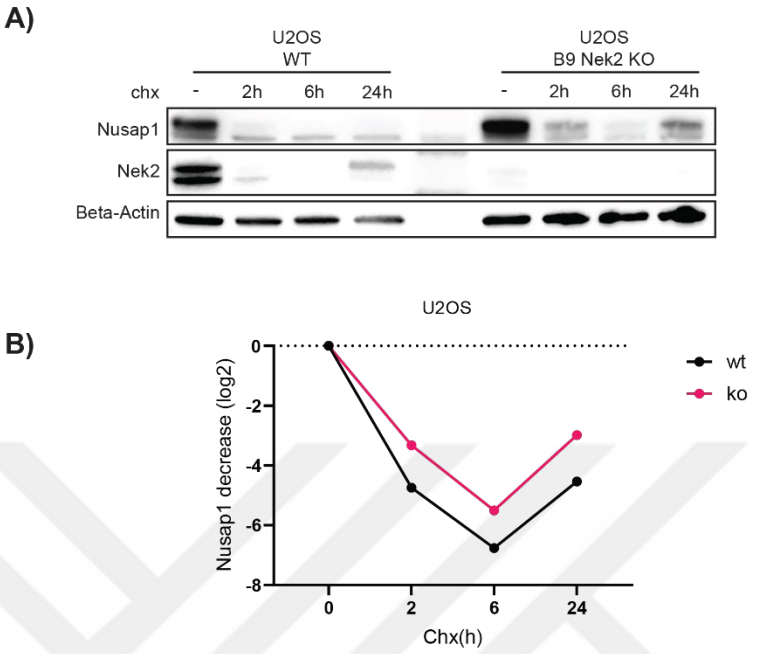

Figure 3-41 Cycloheximide (CHX) chase assay, Nusap1 was more stable at U2OS B9 Nek2KO cell line.

Cells were treated with CHX (10 µM) for 2 h, 6 h, 24 h and blotted with antiNusap1 antibodies. AntiNek2 antibody was used for KO confirmation, anti-Beta-Actin antibody was used for loading control. (A) Nusap1 was more stable at Nek2 KO cell line (B)

Another aspect explored to investigate the proteasomal regulation of Nusap1 involved the use of Mg132, a drug known to inhibit proteasomal degradation. As previously explained, the initial Nek2 overexpression led to a decrease in Nusap1 protein levels within the first 6 hours of doxycycline induction. However, when Nek2-overexpressing cells were treated with Mg132, Nusap1 levels underwent a remarkable recovery, returning to their normal state. This finding suggests that Nek2-mediated proteolysis of Nusap1 can indeed be rescued through Mg132 treatment.

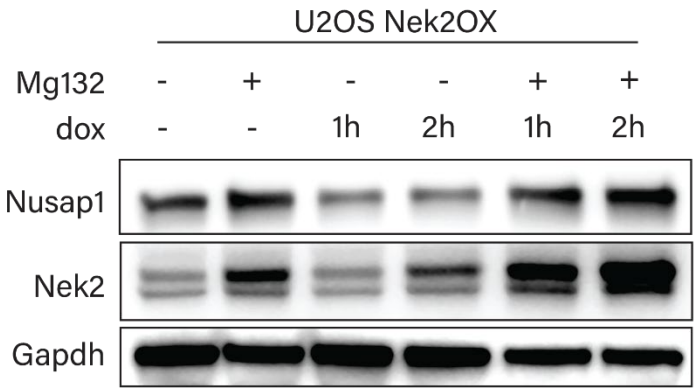

Figure 3-42 Mg132 treatment of Nek2overexpressed groups.
MG132 treatment rescued Nusap1 degradation by Nek2 overexpression.

The ubiquitination process represents a crucial mechanism for the proteasomal degradation of proteins, marking them for ubiquitin-mediated proteolysis. Within this context, the role of Nek2 kinase activity in potentially phosphorylating Nusap1 and triggering its ubiquitination was under investigation. To explore this intriguing phenomenon, a ubiquitination assay was executed.

In this assay, cells were treated with Mg132 for a duration of 5 hours to inhibit proteasomal degradation and accumulate ubiquitinated proteins. Subsequently, Nusap1 was subjected to a pulldown procedure and probed with an anti-ubiquitin antibody. The results unveiled a notable pattern: Nusap1 exhibited reduced ubiquitination levels in U2OS Nek2 knockout (KO) cells when compared to U2OS wild-type (WT) cells.

To perform pulldown of Nusap1, first Nusap1 cDNA was cloned to FLAG tagged viral plasmid. Then, WT and Nek2KO U2OS cell were transduced with viruses packaged with given plasmids.

This outcome suggests a plausible connection between Nek2 kinase activity and the ubiquitination of Nusap1. The reduced ubiquitination observed in Nek2KO cells implies that Nek2 may indeed play a role in promoting the ubiquitination of Nusap1, potentially through its phosphorylation. This finding adds a layer of complexity to our understanding of the regulatory mechanisms governing Nusap1 stability and emphasizes the significance of post-translational modifications in cellular processes.

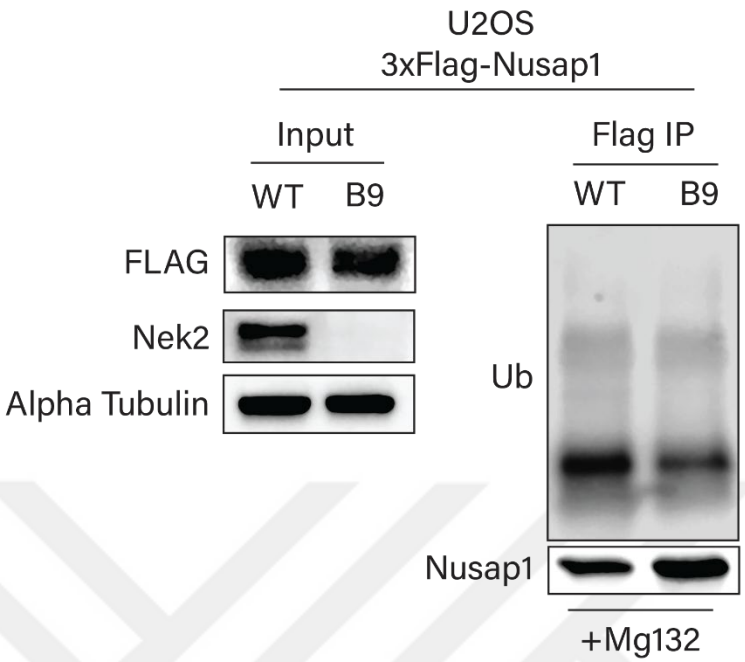

Figure 3-43 Nusap1 was more ubiquitylated in U2OS Nek2WT cellscompared to U2OS B9 Nek2KO cells.

Nusap1 overexpressing cells were treated with Mg132 for 4 hours, then coimmunoprecipitatedby using FLAG-Nusap1 . The protein extracts were then blotted for anti-ubiquitin antibody.

3.17 Global Proteomics Analysis of Nek2KO cells

The ubiquitination assay provided compelling evidence of a relationship between Nek2 and the ubiquitination of Nusap1. The observed differences between Nek2KO and WT cells point to the potential involvement of Nek2 kinase activity in modulating the ubiquitination and subsequent degradation of Nusap1, underscoring the intricate regulatory networks at play in cellular protein dynamics. Therefore, to understand which proteins were affected from Nek2 caused proteasomal degradation, global proteomics analysis was performed for Nek2KO cells.

As anticipated, the experimental results validated our hypotheses regarding the impact of Nek2 on its interacting proteins. Specifically, Nusap1 exhibited upregulation

in Nek2 knockout (Nek2KO) cells, reinforcing Nek2's negative regulatory effect on Nusap1. Conversely, Kif2c protein expression, a recently established Nek2 target, was downregulated in Nek2KO cells, highlighting Nek2's positive regulatory role in modulating Kif2c levels. These findings underscore the multifaceted nature of Nek2's regulatory functions within cellular processes.

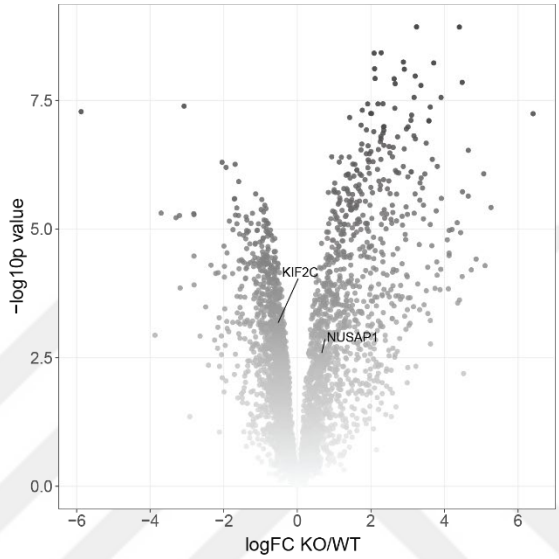

Figure 3-44 Volcano Plot of Mass Spectrometry analysis of U2OS Nek2KO vs WT protein expression change.

Nusap1 was upregulated and Kif2c was downregulated im Nek2KO cells.

Npm1, Cdc26, and Cdc20 were notable proteins that are upregulated in Nek2KO cells. Meanwhile, Anapc1 and Kif2c were downregulated.

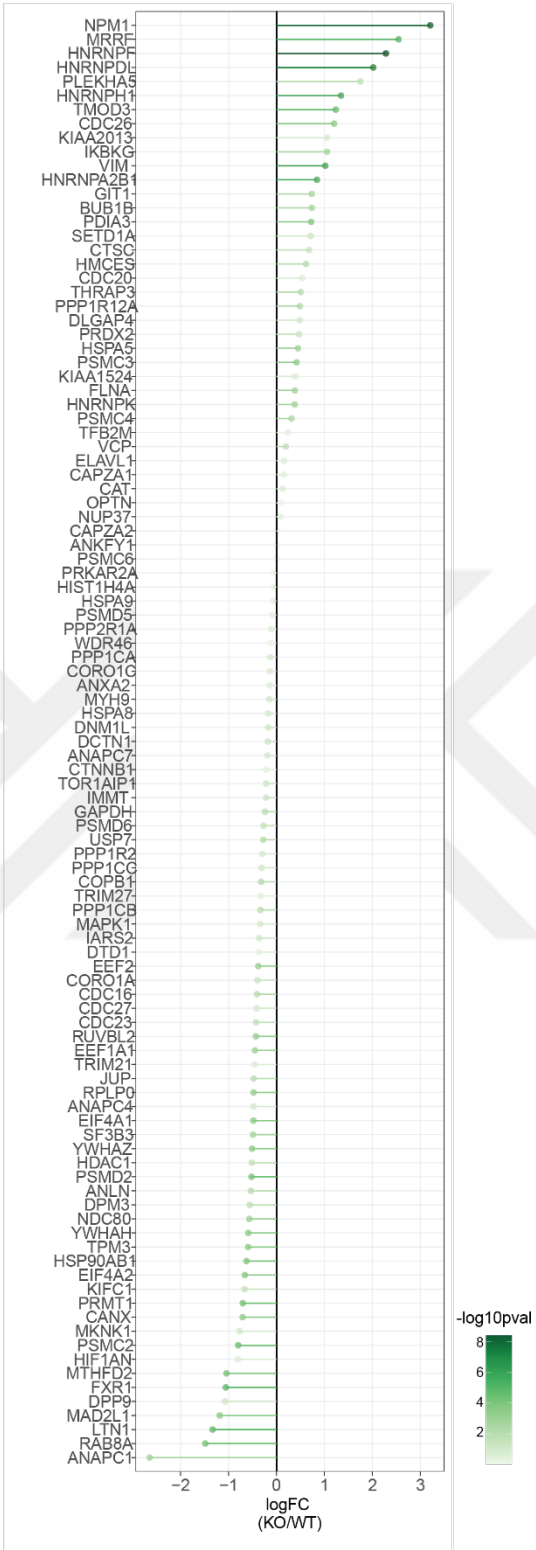

Figure 3-45 Lollipop fold change graph at Nek2KO cell line.

Anapc1 was the most downregulated, meanwhile Npm1 was the most upregulated protein.

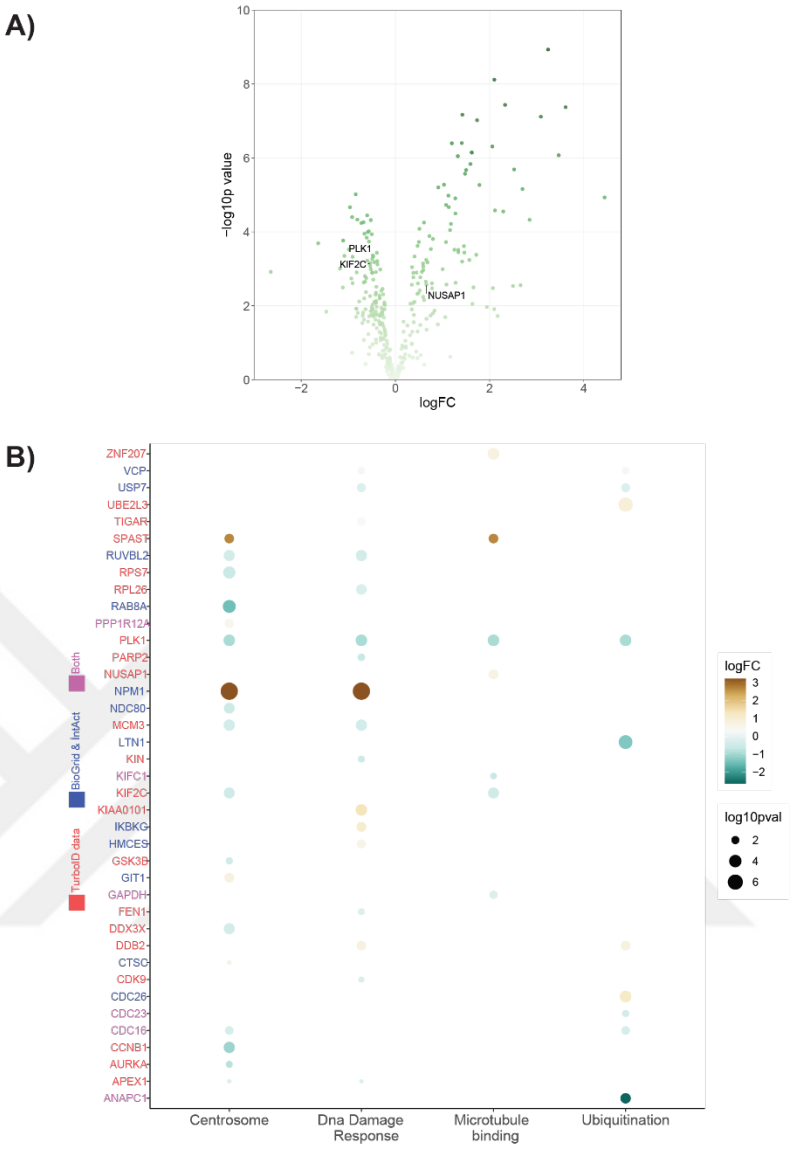

Figure 3-46 Comparison of TurboID data with Nek2KO global proteomics change

(A) Volcano plot of proteins that are in close proximity of Nek2 and detected at Nek2KO global proteomics analysis

(B) Nek2KO fold change of Nek2 interacting proteins (TurboID, Biogrid, IntAct) depending on GO-term of Centrosome, DNA damage response, Microtubule binding, and Ubiquitination.

The comparison of TurboID data with the global proteomics changes observed in Nek2 knockout (Nek2KO) cells provides valuable insights into the interplay between Nek2 and its interacting proteins.

A volcano plot was constructed to visualize the proteins that are in close proximity to Nek2, as identified through TurboID, and their corresponding changes in Nek2KO global proteomics analysis. This plot serves as a comprehensive view of the protein alterations associated with Nek2 proximity. The x-axis typically represents the fold change in protein abundance, while the y-axis signifies the statistical significance of these changes.

In this context, the proteins that are found in proximity to Nek2, as determined by TurboID, are compared with the changes in their expression levels observed in Nek2KO cells. The plot can reveal proteins that show significant alterations in Nek2KO cells, indicating potential interactions or regulatory effects mediated by Nek2.

GO-Terms analysis of these commonly regulated proteins involves assessing the fold changes in the expression levels of Nek2 interacting proteins, as determined by various interaction databases (such as TurboID, Biogrid, and IntAct)/ The GO terms chosen for this analysis include Centrosome, DNA Damage Response, Microtubule Binding, and Ubiquitination.

By categorizing Nek2 interacting proteins based on these specific GO terms, it becomes possible to identify trends in how Nek2 influences proteins associated with these cellular processes. The fold change data in Nek2KO cells allows for the evaluation of Nek2's impact on the regulation of these functional categories.

This comprehensive analysis helps elucidate the broader effects of Nek2 on its interacting proteins, shedding light on the functional pathways and cellular processes that are influenced by Nek2's presence or absence.

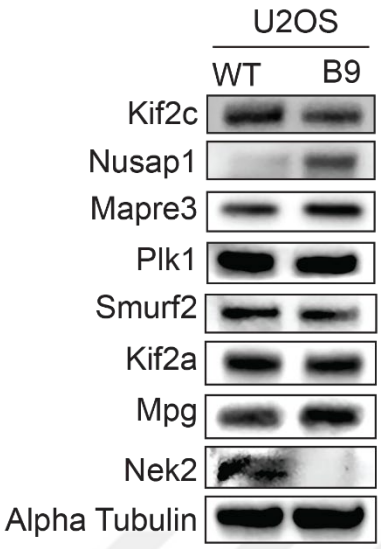

Figure 3-47 Western blot comparison of Target proteins in Nek2KO cell line.

To complement the previous analysis, a Western blot comparison of target proteins in the Nek2 knockout cell line was performed. This additional experimental approach aimed to validate and further characterize the changes observed in the expression levels of specific target proteins in response to Nek2 depletion.

Chapter 4:
CONCLUSION

The study unfolds a multifaceted exploration into the cellular dynamics orchestrated by Nek2, a centrosome-localized kinase with pivotal roles in various cellular processes. Employing the innovative TurboID Proximity Labeling System, this research reveals a vast network of protein interactions associated with Nek2, unveiling its influence across diverse functional contexts. Notably, Nek2 emerges as a central regulator of protein stability, exemplified by its intricate interplay with Nusap1 through ubiquitin-mediated proteolysis. Furthermore, the meticulous validation of these interactions through cycloheximide chase assays, Mg132 treatments, and ubiquitination assays underscores the precision of Nek2's regulatory influence. The deployment of Nek2 knockout cells in conjunction with mass spectrometry and pathway analyses makes clear Nek2's far-reaching impact, both within and beyond the centrosome, encompassing nuclear processes, embryonic development, and signaling regulation. This comprehensive approach enhances our understanding of Nek2's multifaceted functions, marking it as a promising target for therapeutic interventions in cancer and shedding light on the intricate web of protein interactions that govern cellular processes.

Chapter 5:**DISCUSSION**

Our laboratory has unveiled a compelling discovery: Nek2 overexpression triggers the separation of amplified centrosomes, thus inhibiting centrosome clustering in cancer cells. This revelation carries profound implications, suggesting that Nek2 could emerge as a promising target for the development of innovative cancer therapies. However, the precise mechanism through which Nek2 exerts this function and the identities of the proteins it interacts with remain enigmatic. To unravel these mysteries, we have devised a strategy that harnesses the capabilities of the TurboID Proximity Labeling System.

TurboID proximity labelling represents a formidable tool, offering the capacity to unveil the intricate network of proteins that interact with a protein of interest, in this case, Nek2. The methodology involves coupling the target protein (Nek2) with a biotin ligase, which is then expressed within cells. Importantly, only proteins situated in close proximity to Nek2 are biotinylated. These biotinylated proteins can subsequently be isolated and identified.

The concerns about potential unintended activities stemming from the overexpression of engineered proteins in proximity labelling experiments are indeed valid and warrant careful investigation. The comprehensive assessment of potential unintended effects of Nek2 overexpression in this study yielded reassuring results (Naro et al, 2013). Both centrosome separation and cell cycle progression were carefully evaluated, and the data indicated that Nek2 overexpression, in the context of this experiment, did not lead to significant functional irregularities beyond the intended proximity labelling effect. This careful scrutiny of unintended effects is vital for ensuring the reliability and interpretability of experimental outcomes when working with engineered proteins.

The combined findings from mass spectrometry, pathway analysis, and protein enrichment comparisons emphasize that the composition and interactions of Nek2WT and Nek2KD remain largely constant. This suggests that Nek2's kinase activity has limited influence on its association with other proteins and its position.

The cellular component and biological process analyses conducted in this study shed light on the intricate network of protein interactions and functions associated with Nek2, a centrosome-localized kinase with critical roles in various cellular processes, including cell cycle regulation and centrosome dynamics. These analyses provided

valuable insights into the diverse functional contexts in which Nek2 operates, revealing both expected and unexpected enrichments:

The enrichment of proteins related to spindle poles, centrosomes, and microtubules is consistent with Nek2's known localization and functions. (Naro et al, 2013). This reaffirms the reliability of the TurboID strategy in capturing Nek2's centrosomal interactome.

The enrichment of proteins related to the lamin complex and DNA replication complex highlights a nuclear context for Nek2's activity. This suggests that Nek2 may have roles beyond the centrosome, potentially influencing nuclear processes such as DNA replication and structural organization.

The enrichment of proteins associated with the kinetochore complex aligns with the well-established role of Nek2 in regulating kinetochore functions during cell division.

The enrichment of proteins involved in cytoskeleton polarity and microtubule binding is consistent with Nek2's centrosomal localization and its influence on microtubule dynamics. These enrichments underscore Nek2's role in regulating microtubules and cytoskeletal organization.

The enrichment of proteins involved in ubiquitin mediated proteolysis might hint Nek2 kinase activity over proteasomal degradation.

The unexpected enrichment related to membrane assembly in embryonic body morphogenesis suggests a potential novel function for Nek2 beyond its previously recognized roles. This finding prompts further exploration to uncover the specific mechanisms through which Nek2 may influence membrane assembly during embryonic development. Similarly, the enrichment related to the regulation of Rap protein signal transduction hints at previously unknown signaling functions of Nek2. Investigating Nek2's involvement in Rap protein regulation could unveil new regulatory pathways and cellular processes.

The analysis further focused on enriched proteins within specific GO-Terms, such as Centrosome, Cilia, DNA Damage Response, and Mitotic Spindle, to identify potential targets of Nek2. While Nek2's association with Centrosome, Cilia, and Mitotic Spindle is well-documented, (Kimet al, 2015) the enrichment of proteins related to DNA Damage Response provides an intriguing avenue for future exploration.

In summary, this study not only reaffirms the well-established functions of Nek2 in centrosome-related processes but also suggests novel roles in nuclear processes,

embryonic development, and signaling regulation. The identification of potential targets associated with DNA Damage Response and Protein mediated proteolysis opens new avenues for research, while the network analysis highlights the interconnectedness of Nek2 with its interacting proteins. These findings contribute to a deeper understanding of Nek2's multifaceted functions and its potential implications in various cellular contexts, including cancer. Further investigations into the newly uncovered functions and interactions of Nek2 hold promise for advancing our knowledge of this important kinase.

Our approach is further enriched by performing TurboID labeling at distinct stages of the cell cycle. This dynamic perspective allows us to gain a deeper understanding of Nek2's interaction partners and their functional roles during specific phases of cell division. Through this comprehensive investigation, we aim to uncover the molecular intricacies underpinning Nek2's regulation of centrosome separation and clustering. In doing so, we aspire to not only decipher the fundamental mechanisms at play but also identify potential targets for therapeutic intervention in cancer cells afflicted with amplified centrosomes.

The findings from the fold change comparison of target proteins, as visualized in a heatmap derived from mass spectrometry data across different cell cycle stages, provide intriguing insights into the dynamics of protein interactions with Nek2 during the cell cycle.

The heatmap analysis of target proteins revealed that, in general, their distribution remained relatively stable across the various cell cycle stages. This consistency suggests that a core set of proteins consistently interacts with Nek2 regardless of the specific cell cycle phase. Such stability could indicate the presence of essential regulatory interactions that are maintained throughout the cell cycle.

Notably, Mapre3 and Kif2c stood out as exceptions to the overall trend. These two proteins exhibited different proximity to Nek2 across all cell cycle stages. Understanding the roles of Mapre3 and Kif2c in the context of Nek2's functions during the cell cycle could provide valuable insights into centrosome dynamics and microtubule regulation.

The pathway analysis performed for Nek2WT during G1, S, and G2 phases using the shinyGO tool yielded intriguing results. Enrichment in pathways related to Ribosome, Coronavirus disease, Cell cycle, and Ubiquitin Mediated Proteolysis was

observed across all cell cycle stages, similar to unsynchronized samples. This consistency in enriched pathways implies that Nek2's immediate microenvironment and interactions remain stable throughout the cell cycle as well.

The remarkable stability of enriched pathways suggests that Nek2's functional interactome and associated pathways, undergoes limited changes as the cell progresses through different phases of the cell cycle. This stability in Nek2's microenvironment may indicate the presence of critical regulatory processes that remain constant to ensure proper centrosome function and cell division.

The findings suggest that while the majority of Nek2's interacting proteins maintain consistent interactions across the cell cycle, exceptions like Mapre3 and Kif2c may play specialized roles. The enrichment of specific pathways throughout the cell cycle emphasizes the stability of Nek2's functional environment, which could be crucial for its roles in centrosome regulation and cell cycle progression. Further investigation into the functions and regulation of proteins like Mapre3 and Kif2c may provide deeper insights into Nek2's contributions to these processes.

The confirmation of biotinylation of target proteins in this study presents unique challenges. These challenges stem from the notable differences in biotinylation capabilities and activities between the TurboID-only and Nek2-TurboID constructs.

TurboID, as employed in the study, exhibits a broad distribution throughout the cell, including the nucleus, resulting in the biotinylation of a considerable number of proteins. In contrast, the Nek2-TurboID constructs demonstrate distinct and dramatically lower biotinylation profiles, which necessitates to normalize and accurately compare the biotinylation data.

The workflow for data processing involves imputation to address missing values, particularly in NEK2WT and Nek2KD samples, which exhibit lower biotinylation profiles compared to TurboID-only samples. After imputation, each sample should undergo separate normalization to precisely determine the relative intensity levels between samples.

MaxQuant, a widely utilized software, is employed in this process. It calculates iBAQ (intensity-based absolute quantification) by summing the intensities of all detected peptides for a specific protein and dividing by the total number of peptides. This aids in the removal of contaminants from the data. Subsequently, data was re-normalized based on the median after contaminants were removed.

Following the normalization steps, the data was subjected to statistical analysis, with Limma, which was similiar to a t-test. LFQ (Label-Free Quantification) values, similar in concept to iBAQ, are recalculated for each sample. This recalibration enabled the assessment of relative protein intensities and the generation of reliable insights from the biotinylation data.

Rather than comparing the difference in total biotinylation of target proteins between groups, the comparison was made by fractionating the total biotinylated proteins in each sample. This approach allows for a more precise measurement of specific biotinylated targets across experimental groups. The adoption of ELISA (Enzyme-Linked Immunosorbent Assay) was used for effective normalization. ELISA quantifies the total biotinylation levels across various constructs, aligning with established workflows used for Mass Spec data normalization. This normalization procedure ensured more correct comparisons between different samples.

This innovative strategy was adopted to address the issue of disparate total biotinylated proteins stemming from EV-TurboID samples. By focusing on the proportion of biotinylated target proteins within the context of overall biotinylation, a more comparable and informative assessment was achieved. This approach sought to align the western blot validation process with the principles of mass spectrometry normalization, enabling a more accurate evaluation of the enrichment of the identified target proteins.

Coimmunoprecipitation delved into the direct protein-protein interactions involving Nek2 and its target proteins. Through the judicious use of engineered cells, specialized IP lysis buffers, and fixation methods (PFA and methanol), coimmunoprecipitation experiment effectively unveiled direct bindings between Nek2 and Kif2c, Mapre3, Mpg, Nusap1, and Smurf2. This validation process contributes to a more comprehensive understanding of the network of interactions revolving around Nek2.

The establishment of Nek2KO cell lines marked a critical stride in comprehending the significance of Nek2's presence in various cellular processes. Through the meticulous employment of Crispr-Cas9 technology, followed by a detailed selection and screening regimen, the Nek2KO cell lines, specifically B5 and B9, were identified as vital tools for unraveling the roles and interactions of Nek2 with the designated target proteins. This foundational work holds the potential to yield valuable insights into the intricate mechanisms governing cellular dynamics and regulatory pathways.

Investigation into the regulatory dynamics between Nek2 and Nusap1 offers valuable insights into their functional relationship. The observed trends underscore the intricate nature of cellular regulatory networks and emphasize the need for understanding of protein interactions and their impact on cellular processes. The combination of the cycloheximide chase assay and the Mg132 assay provided compelling evidence for the regulatory role of Nek2 in modulating Nusap1 protein levels through proteasomal degradation pathways. This intricate regulatory mechanism highlights the significance of post-translational modifications and protein stability in cellular processes, shedding light on the dynamic interplay between Nek2 and Nusap1.

The ubiquitination assay provided compelling evidence of a relationship between Nek2 and the ubiquitination of Nusap1. The observed differences between Nek2KO and WT cells point to the potential involvement of Nek2 kinase activity in modulating the ubiquitination and subsequent degradation of Nusap1, underscoring the intricate regulatory networks at play in cellular protein dynamics.

The results of the ubiquitination experiment strongly indicated that Nek2 plays a pivotal role in the regulation of protein degradation, particularly exemplified by its influence on the degradation of specific proteins like Nusap1. The phosphorylation of target proteins by Nek2 appears to be a key event that marks them for ubiquitin-mediated proteolysis. Interestingly, a recent study revealed that Ola1 protein is ubiquitinylated by Aurora A due to Nek2 phosphorylation (Fang et al., 2023). This post-translational modification, orchestrated by Nek2, potentially serves as a critical regulatory mechanism in the cell.

To go deeper into this mechanism and identify potential target proteins, another comprehensive mass spectrometry analysis was undertaken. This time, the global proteomics of Nek2 knockout (Nek2KO) cells were compared to the proteomics analysis conducted using the TurboID proximity labelling system. The focus was on identifying common proteins that not only reside in close proximity to Nek2 but are also influenced by the depletion of Nek2.

The comparison of TurboID data with Nek2KO global proteomic changes provides understanding of the relationships between Nek2 and its interacting proteins. It allows for the identification of proteins with altered expression patterns in Nek2KO cells and offers insights into the functional categories influenced by Nek2's regulatory roles.

BIBLIOGRAPHY

Fang, Z., Li, X., Yoshino, Y., Suzuki, M., Qi, H., Hinari Murooka, … Chiba, N. (2023). Aurora A polyubiquitinates the BRCA1-interacting protein OLA1 to promote centrosome maturation. *Cell Reports*, *42*(8), 112850–112850. https://doi.org/10.1016/j.celrep.2023.112850

Tiengo, A., Barbarini, N., Troiani, S. et al (2009). A Perl procedure for protein identification by Peptide Mass Fingerprinting. BMC Bioinformatics 10 (Suppl 12), S11. https://doi.org/10.1186/1471-2105-10-S12-S11

Turriziani, Benedetta & Garcia-Munoz, Amaya & Pilkington, Ruth & Raso, Cinzia & Kolch, Walter & Kriegsheim, Alexander. (2014). On-Beads Digestion in Conjunction with Data-Dependent Mass Spectrometry: A Shortcut to Quantitative and Dynamic Interaction Proteomics. Biology. 3. 320-32. 10.3390/biology3020320.

Schwanhäusser, B., Busse, D., Li, N. et al. (2011) Global quantification of mammalian gene expression control. Nature 473, 337–342. https://doi.org/10.1038/nature10098

Bahe, S., Stierhof, Y.-D., Wilkinson, C. J., Leiss, F., & Nigg, E. A. (2005). Rootletin forms centriole-associated filaments and functions in centrosome cohesion. Journal of Cell Biology, 171(1), 27–33. https://doi.org/10.1083/jcb.200504107

Bahmanyar, S., Kaplan, D. D., DeLuca, J. G., Giddings, T. H., O'Toole, E. T., Winey, M., Salmon, E. D., Casey, P. J., Nelson, W. J., & Barth, A. I. M. (2007). β-Catenin is a Nek2 substrate involved in centrosome separation. Genes & Development, 22(1), 91–105. https://doi.org/10.1101/gad.1596308

Béganton, B., Solassol, I., Mangé, A., & Solassol, J. (2019). Protein interactions study through proximity-labeling. Expert Review of Proteomics, 16(8), 717–726. https://doi.org/10.1080/14789450.2019.1638769

Carolina, I., Peres, A., Rafael, P., Fernanda Luisa Basei, Luidy Kazuo Issayama, Camila, … Jörg Kobarg. (2021). On Broken Ne(c)ks and Broken DNA: The Role of Human NEKs in the DNA Damage Response. *Cells*, *10*(3), 507–507. https://doi.org/10.3390/cells10030507

Choi, B., Tajhal Dayaram, Parikh, N., Wilkins, A. D., Nagarajan, M., Novikov, I. B., … Weber, G. (2018). Literature-based automated discovery of tumor suppressor p53 phosphorylation and inhibition by NEK2. Proceedings of the National Academy of Sciences of the United States of America, 115(42), 10666–10671. https://doi.org/10.1073/pnas.1806643115

Cheerambathur, D. K., Prevo, B., Chow, T.-L., Hattersley, N., Wang, S., Zhao, Z., Kim, T., Gerson-Gurwitz, A., Oegema, K., Green, R., & Desai, A. (2019). The Kinetochore-Microtubule Coupling Machinery Is Repurposed in Sensory Nervous System Morphogenesis. Developmental Cell, 48(6), 864-872.e7. https://doi.org/10.1016/j.devcel.2019.02.002

Cosenza, M. R., Cazzola, A., Rossberg, A., Schieber, N. L., Konotop, G., Bausch, E., Slynko, A., Holland-Letz, T., Raab, M. S., Dubash, T., Glimm, H., Poppelreuther, S., Herold-Mende, C., Schwab, Y., & Krämer, A. (2017). Asymmetric Centriole Numbers at Spindle Poles Cause Chromosome Missegregation in Cancer. Cell Reports, 20(8), 1906–1920. https://doi.org/10.1016/j.celrep.2017.08.005

Didusch, S., Madern, M., Hartl, M., & Baccarini, M. BMC Genomics 23, 817 (2022). amica: an interactive and user-friendly web-platform for the analysis of proteomics data. DOI: https://doi.org/10.1186/s12864-022-09058-7.

Fang, Y., & Zhang, X. (2016). Targeting NEK2 as a promising therapeutic approach for cancer treatment. Cell Cycle, 15(7), 895–907. https://doi.org/10.1080/15384101.2016.1152430

Firat-Karalar, E., Rauniyar, N., Yates, John R., & Stearns, T. (2014). Proximity Interactions among Centrosome Components Identify Regulators of Centriole Duplication. Current Biology, 24(6), 664–670. https://doi.org/10.1016/j.cub.2014.01.067

Fry, A. M. (1998). A centrosomal function for the human Nek2 protein kinase, a member of the NIMA family of cell cycle regulators. The EMBO Journal, 17(2), 470–481. https://doi.org/10.1093/emboj/17.2.470

Fu, J., Hagan, I. M., & Glover, D. M. (2015). The centrosome and its duplication cycle. Cold Spring Harbor perspectives in biology, 7(2), a015800. https://doi.org/10.1101/cshperspect.a015800

Fukasawa K. (2005). Centrosome amplification, chromosome instability and cancer development. Cancer letters, 230(1), 6–19. https://doi.org/10.1016/j.canlet.2004.12.028

Gupta, Gagan D., Coyaud, É., Gonçalves, J., Mojarad, Bahareh A., Liu, Y., Wu, Q., Gheiratmand, L., Comartin, D., Tkach, Johnny M., Cheung, Sally W. T., Bashkurov, M., Hasegan, M., Knight, James D., Lin, Z.-Y., Schueler, M., Hildebrandt, F., Moffat, J., Gingras, A.-C., Raught, B., & Pelletier, L. (2015). A Dynamic Protein Interaction Landscape of the Human Centrosome-Cilium Interface. Cell, 163(6), 1484–1499. https://doi.org/10.1016/j.cell.2015.10.065

Han, X., Aslanian, A., & Yates, J. R. (2008). Mass spectrometry for proteomics. Current Opinion in Chemical Biology, 12(5), 483–490. https://doi.org/10.1016/j.cbpa.2008.07.024

Job, D., Valiron, O., & Oakley, B. (2003). Microtubule nucleation. Current opinion in cell biology, 15(1), 111–117. https://doi.org/10.1016/s0955-0674(02)00003-0

Kim, S., Lee, K.-W., Choi, J.-H., Ringstad, N., & Brian David Dynlacht. (2015). Nek2 activation of Kif24 ensures cilium disassembly during the cell cycle. *Nature Communications*, *6*(1). https://doi.org/10.1038/ncomms9087

Kleylein-Sohn, J., Westendorf, J., Le Clech, M., Habedanck, R., Stierhof, Y.-D., & Nigg, E. A. (2007). Plk4-Induced Centriole Biogenesis in Human Cells. Developmental Cell, 13(2), 190–202. https://doi.org/10.1016/j.devcel.2007.07.002

Lee, J., & Gollahon, L. (2013). Mitotic perturbations induced by Nek2 overexpression require interaction with TRF1 in breast cancer cells. Cell Cycle, 12(23), 3599–3614. https://doi.org/10.4161/cc.26589

Lin, A. (2015). Direct ELISA. *Methods in Molecular Biology*, 61–67. https://doi.org/10.1007/978-1-4939-2742-5_6

Lou, Y., Yao, J., Zereshki, A., Dou, Z., Ahmed, K., Wang, H., Hu, J., Wang, Y., & Yao, X. (2004). NEK2A Interacts with MAD1 and Possibly Functions as a Novel Integrator of the Spindle Checkpoint Signaling. Journal of Biological Chemistry, 279(19), 20049–20057. https://doi.org/10.1074/jbc.m314205200

Man, X., Megraw, T. L., & Lim, Y. P. (2015). Cep68 can be regulated by Nek2 and SCF complex. European Journal of Cell Biology, 94(3-4), 162–172. https://doi.org/10.1016/j.ejcb.2015.01.004

Mardin, Balca R., Agircan, Fikret G., Lange, C., & Schiebel, E. (2011). Plk1 Controls the Nek2A-PP1γ Antagonism in Centrosome Disjunction. Current Biology, 21(13), 1145–1151. https://doi.org/10.1016/j.cub.2011.05.047

Marina, M. (2014). Nek2 and Plk4: prognostic markers, drivers of breast tumorigenesis and drug resistance. Frontiers in Bioscience, 19(2), 352. https://doi.org/10.2741/4212

Mittal, K., Kaur, J., Jaczko, M., Wei, G., Toss, M. S., Rakha, E. A., Janssen, E. A. M., Søiland, H., Kucuk, O., Reid, M. D., Gupta, M. V., & Aneja, R. (2020). Centrosome amplification: a quantifiable cancer cell trait with prognostic value in solid malignancies. Cancer and Metastasis Reviews, 40(1), 319–339. https://doi.org/10.1007/s10555-020-09937-z

Naro, C., Barbagallo, F., Paolo Chieffi, Bourgeois, C. F., Maria Paola Paronetto, & Sette, C. (2013). The centrosomal kinase NEK2 is a novel splicing factor kinase involved in cell survival. *Nucleic Acids Research*, *42*(5), 3218–3227. https://doi.org/10.1093/nar/gkt1307

Neagu, A.-N., Jayathirtha, M., Baxter, E., Donnelly, M., Petre, B. A., & Darie, C. C. (2022). Applications of Tandem Mass Spectrometry (MS/MS) in Protein Analysis for

Nigg, E. A. (2002). Centrosome aberrations: cause or consequence of cancer progression? Nature Reviews Cancer, 2(11), 815–825. https://doi.org/10.1038/nrc924

Nigg, E. A., & Stearns, T. (2011). The centrosome cycle: Centriole biogenesis, duplication and inherent asymmetries. Nature cell biology, 13(10), 1154–1160. https://doi.org/10.1038/ncb2345

Proteins Required for Centrosome Clustering in Cancer Cells. (2023). Science Translational Medicine. https://www.science.org/doi/10.1126/scitranslmed.3000915

Roberts, M. S., Sahni, J. M., Schrock, M. S., Piemonte, K. M., Weber-Bonk, K. L., Seachrist, D. D., Avril, S., Anstine, L. J., Singh, S., Sizemore, S. T., Varadan, V., Summers, M. K., & Keri, R. A. (2020). LIN9 and NEK2 Are Core Regulators of Mitotic Fidelity That Can Be Therapeutically Targeted to Overcome Taxane Resistance. Cancer Research, 80(8), 1693–1706. https://doi.org/10.1158/0008-5472.can-19-3466

Silkworth, W. T., Nardi, I. K., Paul, R., Mogilner, A., & Cimini, D. (2012). Timing of centrosome separation is important for accurate chromosome segregation. Molecular Biology of the Cell, 23(3), 401–411. https://doi.org/10.1091/mbc.e11-02-0095

Schatten H. (2008). The mammalian centrosome and its functional significance. Histochemistry and cell biology, 129(6), 667–686. https://doi.org/10.1007/s00418-008-0427-6

Trinkle-Mulcahy, L. (2019). Recent advances in proximity-based labeling methods for interactome mapping. F1000Research, 8, 135. https://doi.org/10.12688/f1000research.16903.1

Ohta, M., Watanabe, K., Ashikawa, T., Nozaki, Y., Yoshiba, S., Kimura, A., & Kitagawa, D. (2018). Bimodal Binding of STIL to Plk4 Controls Proper Centriole Copy Number. Cell Reports, 23(11), 3160-3169.e4. https://doi.org/10.1016/j.celrep.2018.05.030

Ozkan, N. E., Yigit, B. N., Degirmenci, B. S., Qureshi, M. H., Yapici, G. N., Kamacıoglu, A., Bavili, N., Kiraz, A., & Ozlu, N. (2023). Cell cycle-dependent palmitoylation of protocadherin 7 by ZDHHC5 promotes successful cytokinesis. *Journal of cell science*, *136*(6), jcs260266. https://doi.org/10.1242/jcs.260266

WeiqiangChen. (2023). moritzmadern/Cassiopeia_LFQ: Read contaminant.fasta instead of con_table.txt. *Zenodo*. https://doi.org/10.5281/zenodo.7728855

Winey, M., & O'Toole, E. (2014). Centriole structure. Philosophical transactions of the Royal Society of London. Series B, Biological sciences, 369(1650), 20130457. https://doi.org/10.1098/rstb.2013.0457